

**Title:** Localization of HET-S to the cell periphery, and not to [Het-s] aggregates, is associated with [Het-s]-HET-S toxicity

**Authors:** Vidhu Mathur<sup>1</sup>, Carolin Seuring<sup>2</sup>, Roland Riek<sup>2</sup>, Sven J. Saupe<sup>3</sup> and Susan W. Liebman<sup>1</sup>

**Affiliations:** <sup>1</sup> Department of Biological Sciences, University of Illinois at Chicago, Chicago, IL 60607, USA. <sup>2</sup> Institute of Physical Chemistry, ETH Zurich, CH-8093 Zurich, Switzerland, <sup>3</sup> Laboratoire de Génétique Moléculaire des Champignons, IBGC UMR CNRS 5095, Université de Bordeaux 2, 33077 Bordeaux, France

**Contact:** [suel@uic.edu](mailto:suel@uic.edu)/[sliebman@unr.edu](mailto:sliebman@unr.edu)

**Running Title:** [Het-s]/HET-S toxicity

## **Abstract**

Prion diseases are associated with accumulation of the amyloid form of the prion protein, but the mechanisms of toxicity are unknown. Amyloid toxicity is also associated with fungal prions. In *Podospora anserina*, the simultaneous presence of [Het-s] prion and its allelic protein HET-S causes cell death in a self/non-self discrimination process. Here, using the prion form of a fragment of HET-s ( $[PrD_{157}^+]$ ), we show that [Het-s]/HET-S toxicity can be faithfully recapitulated in yeast. Overexpression of Hsp40 chaperone, Sis1, rescues this toxicity by curing cells of  $[PrD_{157}^+]$ . We find no evidence for toxic  $[PrD_{157}^+]$  conformers in the presence of HET-S. Instead,  $[PrD_{157}^+]$  appears to seed HET-S to accumulate at the cell periphery and to form aggregates distinct from visible  $[PrD_{157}^+]$  aggregates. Furthermore, HET-S mutants that cause HET-S to be sequestered into  $[PrD_{157}^+]$  prion aggregates are not toxic. The localization of HET-S at the cell periphery and its association with cell death was also observed in the native host *Podospora anserina*. Thus, upon interaction with [Het-s], HET-S localizes to the cell periphery and this re-localization, rather than the formation of mixed HET-s/HET-S aggregates, is associated with toxicity.

## **Introduction**

Amyloids are insoluble,  $\beta$ -sheet rich proteins, the accumulation of which can sometimes lead to disease. For example, Alzheimer's, Huntington's and Parkinson's diseases are respectively associated with the accumulation of A $\beta$ , mutant Htt1 and  $\alpha$ -synuclein deposits, in the brain (2). Prions are infectious amyloids. In mammals, prion

disease is associated with conversion of soluble prion protein, PrP<sup>C</sup>, into an insoluble, aggregated prion form, PrP<sup>Sc</sup> (1, 45).

Prions in yeast and fungi are attractive candidates to study prion biology. They are responsible for certain heritable traits (59) and, like the mammalian prion, are infectious amyloids (8, 34, 37, 44, 58). While mammalian prion diseases cause neurodegeneration associated with accumulation of PrP<sup>Sc</sup>, yeast and fungal prions are toxic only under certain conditions. [PSI<sup>+</sup>], the prion form of the yeast translation termination factor Sup35, is toxic when Sup35 is overexpressed, due to the sequestration of the essential translation termination factor, Sup45, into the large Sup35 aggregates (9, 17, 21, 54). Also, the yeast [PIN<sup>+</sup>] prion (prion form of Rnq1 protein of unknown function) is toxic when Rnq1 is overexpressed (24). This toxicity is due to the accumulation of soluble toxic oligomeric Rnq1 which can be recruited into the nucleus, and converted to harmless amyloid by overexpressing the Hsp40 chaperone, Sis1 (23). The [Het-s] prion of the filamentous fungus *Podospora anserina* is toxic in the presence of the allelic HET-S (big S) non-prion protein, but the mechanism of this toxicity is unknown.

The [Het-s] prion forms an amyloid that functions in heterokaryon incompatibility in *Podospora* (14). Heterokaryon incompatibility is a self/non-self recognition process that occurs when vegetative hyphae with different *het* alleles fuse (47, 48). The fusion of hyphae with unlike *het*-genotype leads to death. Incompatibility appears to be advantageous because it limits cytoplasmic exchange between unlike individuals and thus reduces horizontal transmission of mycoviruses and other deleterious cytoplasmic replicons.

The *het-s* locus, which has two alternate alleles: *het-s* (little s) and *het-S* (big S), is one of nine heterokaryon incompatibility loci in *Podospora* and is the only locus that involves a prion. Both HET-s and HET-S proteins are 289 amino acids long and differ in only 13 amino acids. The HET-s protein can exist in either a soluble, non-prion form, [Het-s\*], or an aggregated, prion form, [Het-s] (14). A fusion of non-prion [Het-s\*] cells and HET-S containing cells is viable, while a fusion between prion [Het-s] and HET-S cells is lethal (14).

The C-terminal 218-289 amino acids (aas) of HET-s, called the prion domain (PrD) (Figure 1A), are necessary and sufficient for prion formation and propagation in *Podospora*, or in yeast and for amyloid formation *in vitro* (5, 13, 22, 53). The N-terminal 1-227 aas comprise a structured globular domain (called HeLo domain, Figure 1A) which determines if the protein is HET-s or HET-S (5, 28). In *Podospora*, the PrD from either HET-s or HET-S is able to form a prion (4), however only the HET-s (and not HET-S) full length allele is able to do so, indicating that the HET-S HeLo domain inhibits PrD prion formation *in cis*. Additionally, *in vitro*, HET-S inhibits HET-s PrD amyloid assembly *in trans* (28).

While the full length [Het-s] prion is toxic with HET-S, the prion form of HET-s PrD fused to GFP shows only a partial incompatibility (4). However, a slightly larger fragment of HET-s containing aas 157-289 (called PrD<sub>157</sub> here) is capable of forming a prion with the entire incompatibility response of the full length HET-s protein (Figure 1A) (4).

It was recently shown that HET-S does not self-aggregate, nor can it be seeded to aggregate by [Het-s] fibers *in vitro*. However, HET-S was shown to co-aggregate with

the [Het-s] prion in *Podospora* and genetic evidence suggests that the  $\beta$ -solenoid folding of the HET-S PrD region is required for HET-S induced toxicity. It was proposed that the amyloid folding of the HET-S PrD region induced by interaction with [Het-s] triggers an un/refolding of the HeLo globular domain that depends upon the overlap between the PrD and HeLo domains, and involves HeLo domain dimerization (28). How this HET-S HeLo domain refolding brings about toxicity is unknown.

HET-S associated toxicity is of particular interest as it is an example of a purposeful, biologically relevant mechanism of amyloid-related toxicity. In this system, amyloid-related toxicity is not to be understood simply as a pathological event, but as an integrated biological process.

Here, using yeast and *Podospora*, we implicate HET-S aggregation, rather than the formation of a toxic [Het-s] species, in toxicity. While HET-S was previously shown to be sequestered into [Het-s] prion foci (28), we now show that such HET-S aggregation is not associated with toxicity. Rather, in both yeast and *Podospora*, toxicity is associated with accumulation of HET-S at the cell periphery and a new type of HET-S aggregate in a form that is distinct from visible [*PrD*<sub>157</sub><sup>+</sup>] or [Het-s] foci.

## **Materials and methods**

### **Yeast strains and plasmids**

The yeast strains used were: L1749 (*MATa ade1-14 ura3-52 leu2-3,112 trp1-289 his3-200 [psi<sup>-</sup>][PIN<sup>+</sup>]*), L1763 (*MATa ade1-14 ura3-52 leu2-3,112 trp1-289 his3-200 [PSI<sup>+</sup>][pin<sup>-</sup>]*), L1753 (*MATa ade1-14 ura3-52 leu2-3,112 trp1-289 lys9-A21 [psi<sup>-</sup>][PIN<sup>+</sup>]*), L2910 (*MATa ade1-14 ura3-52 leu2-3,112 trp1-289 his3-200 [psi<sup>-</sup>][pin<sup>-</sup>]*) and GF727 (*MATa ade2-1 his3 $\Delta$ 202 leu2 $\Delta$ 1 trp1 $\Delta$ 63 ura3-52 kar1-1 [psi<sup>-</sup>][PIN<sup>+</sup>]*). Yeast was grown

in synthetic or complex, solid or liquid, media at 30°C (50). Plasmid selective synthetic media were used unless otherwise mentioned. Galactose media had 2 % raffinose + 2 % galactose (2 % gal). Plasmids with *URA3* were lost by plating cells on synthetic solid media containing 1 mg/ml 5- fluoro orotic acid (5-FOA) (7). Plasmids with other markers were lost by 3 consecutive passes of cells on non-selective media. Plasmid loss was confirmed by the absence of growth on media lacking the plasmid marker.

The plasmids used are listed in Table 1. All plasmids were constructed by placing the respective genes in pRS vectors with *GPD* or *GALI* promoters. pGPD-PrD<sub>157</sub>-GFP (p1587) was made by cloning the fusion PrD<sub>157</sub>-GFP into p426GPD. p1587H was made by changing *URA3* (in p1587) to *HIS3* using the marker swap plasmid pUH7 (16). HET-S-HA (p1841) was constructed by adding the sequence of a single HA peptide in-frame with the HET-S sequence at the C-terminus: the HET-S-HA PCR construct was then cloned into pRS314*GAL* under the *GALI* promoter. The DsRed fusions were made by putting the gene of interest in frame with DsRed in p1692. The HET-S E86K and T266P mutations were made in p1841 and p1842 with site directed PCR using the Stratagene Quikchange II kit. NM-HET-S/s (1-227) (p1849 and p1851) and HET-S/s (1-227)-Rnq1PD were made by cloning HET-S (or HET-s) aas 1-227 in-frame with Sup35NM at the C-terminus or Rnq1 (176-405) at the N-terminus.

### **Construction of [*PrD*<sup>+</sup>] and [*PrD*<sub>157</sub><sup>+</sup>] cultures**

[*PrD*<sup>+</sup>] cells were obtained by transforming pGPD-PrD-GFP (p1920) into [*psi*<sup>-</sup>] [*PIN*<sup>+</sup>] cells (L1749). Transformants were grown and cells with rings were micromanipulated to give rise to [*PrD*<sup>+</sup>] cultures with cells containing two dot aggregates.

The [*PrD*<sub>157</sub><sup>+</sup>] strain was made by co-transforming pGPD-PrD<sub>157</sub>-GFP (p1587H, *HIS3*) and pGPD-HET-s PrD (p1389, *URA3*) plasmids into [*psi*<sup>-</sup>][*PIN*<sup>+</sup>] (L1749) cells (Figure 1B). Transformants were allowed to grow on selective media and cells with fluorescent dots were micromanipulated to form colonies. Finally, the HET-s PrD plasmid was lost by streaking on 5-FOA plates. His<sup>+</sup> Ura<sup>-</sup> colonies were [*PrD*<sub>157</sub><sup>+</sup>] and maintained PrD<sub>157</sub>-GFP aggregates in 100 % of the cells after 15 generations. Unseeded PrD<sub>157</sub>-GFP (never transformed with pGPD-PrD) in L1749 was [*prd*<sub>157</sub><sup>-</sup>] and showed diffuse PrD<sub>157</sub>-GFP.

### Biochemical analyses

[*PrD*<sub>157</sub><sup>+</sup>] or [*prd*<sub>157</sub><sup>-</sup>] cells containing HET-S plasmid or vector were grown in 50-600 ml synthetic dextrose medium to late log phase, washed twice with water and inoculated in 50-600 ml synthetic medium with 2 % gal to induce HET-S. Cells were harvested after 4-8 hrs of induction. Lysis and co-immunocapture were as described previously (39).

For high speed centrifugation analysis, lysates were cleared with two spins at 600 x g for 1 min. Normalized total protein lysates (1 mg/ml) were centrifuged at 100,000g for 30 mins. The supernatant and pellet were separated, boiled in sample buffer with 2 % SDS for 10 mins and analyzed by SDS-PAGE and Western blotting.

To visualize detergent-resistant oligomers, 10-40 µg (or 100 µg for SDD-AGE (3)) of total protein extracts were treated with 2 % SDS (or 2 % sarkosyl for SDD-AGE) containing sample buffer for 10 mins at room temperature, run on 10 % acrylamide (or 1.5 % agarose for SDD-AGE) gels and analyzed by Western blotting.

For gel filtration analysis, crude lysates were loaded on a Superose 6.0 column (GE Healthcare). About 30 fractions (0.7-1.4 ml) were collected and precipitated by incubating at 4°C overnight with 20 % TCA. Fractions were then spun at maximum speed for 5 mins, washed thrice with acetone, dried, treated with 2 % SDS sample buffer at room temperature, loaded on two 15 well gels serially and analyzed by Western blotting

Anti-HA antibody was from Sigma. Anti-GFP antibody was from Roche Applied Sciences.

### **Fluorescence microscopy**

For yeast mating experiments, HET-S-DsRed wild type (p1842) or mutants (p1884 and p1886) in L1753 or GF727 (*MAT $\alpha$* ) was induced by growth in liquid, plasmid selective, synthetic 2 % gal medium overnight. These cells were mated with *MAT $\alpha$*  [*PrD<sub>157</sub><sup>+</sup>*] and [*prd<sub>157</sub><sup>-</sup>*] cells on complex 2 % gal plates and fused cells/zygotes were visualized after 4 or 8 hrs. The colocalization images were collected as Z-stacks and subjected to 3D deconvolution on a Zeiss Axiovert 200M equipped with a digital camera.

When showing that HET-S does not inhibit newly synthesized PrD<sub>157</sub> protein from joining pre-existing [*PrD<sub>157</sub><sup>+</sup>*] aggregates, soluble/unaggregated PrD<sub>157</sub>-DsRed was quantified using Alpha Imager software. In HET-S or vector expressing cells (at least 20 cells each), random areas of equal sizes that did not contain prion aggregates were selected and fluorescence was measured in random units using the SpotDenso in AlphaImager program and was normalized to the background. The difference between average fluorescence intensities with and without HET-S expression was found to be insignificant.

A *Podospora anserina*  $\Delta$ *het-s* strain was transformed either with a plasmid expressing a HET-s-RFP fusion protein (28) or a HET-S-GFP fusion protein (13). The strains were then co-inoculated on solid medium and grown for 24 hrs at 25°C and the mycelia were analyzed by fluorescence microscopy in the [Het-s]/[Het-S] confrontation zone where incompatible cell fusion took place.

## **Results**

### **PrD<sub>157</sub>-GFP can form a prion in yeast**

We previously showed that at a low level of expression, the P<sub>GALI</sub>-PrD-GFP fusion remained diffuse (previously called [het-s]<sub>y</sub>, now called [*prd*]), but a high level of expression of P<sub>GALI</sub>-PrD-GFP caused the formation of fluorescent rings followed by stable propagation of two fluorescent dots in daughter cells even when expression of PrD-GFP was reduced to the original low level (39, 53). The cells in this state, previously called [Het-s]<sub>y</sub>, are now called [*PrD*<sup>+</sup>]. Likewise, when we expressed PrD-GFP with the strong *GPD* promoter, it spontaneously induced prion rings followed by two dot aggregates in daughters. However, since we could not reduce the level of PrD-GFP with this promoter, we could not obtain pure non-prion [*prd*] cells.

Thus, to recapitulate [Het-s]/HET-S toxicity in yeast in which we planned to overexpress HET-S from the *GALI* promoter, we took advantage of the extended HET-s PrD fragment (aas 157-289), called PrD<sub>157</sub> here, which forms a prion that is toxic with HET-S in *Podospora* (4). In contrast to HET-s PrD-GFP, the HET-s PrD<sub>157</sub>-GFP fragment, highly expressed from the efficient *GPD* promoter, remained diffuse in yeast. However, PrD<sub>157</sub>-GFP did form fluorescent foci when co-overexpressed with untagged PrD and the daughter cells continued to propagate these foci efficiently even when HET-s

PrD was lost (Figure 1B). We designate cells propagating fluorescent PrD<sub>157</sub>-GFP foci as [*PrD*<sub>157</sub><sup>+</sup>] and those with unaggregated, diffuse PrD<sub>157</sub>-GFP as [*prd*<sub>157</sub><sup>-</sup>]. As expected for a prion, transfer (cytoduction) of [*PrD*<sub>157</sub><sup>+</sup>] donor cytoplasm into [*prd*<sub>157</sub><sup>-</sup>] frequently transferred the [*PrD*<sub>157</sub><sup>+</sup>] state: 54.8 % of cytoduced recipients became [*PrD*<sub>157</sub><sup>+</sup>] compared to 0 % when a [*prd*<sub>157</sub><sup>-</sup>] strain was used as a donor.

While both [*PrD*<sup>+</sup>] and [*PrD*<sub>157</sub><sup>+</sup>] propagate as prions in yeast, their aggregates have distinct properties. PrD-GFP (expressed from *GPD* or *GALI* promoter) propagates as two dot aggregates (39, 53), however PrD<sub>157</sub>-GFP formed single to multiple-dots per cell (Figure 1B). Moreover, [*PrD*<sub>157</sub><sup>+</sup>] aggregates break down into SDS-resistant oligomers (not shown), while [*PrD*<sup>+</sup>] aggregates are monomerized by SDS, but form oligomers in the presence of a milder detergent, sarkosyl (53). Finally, the presence of [*PrD*<sup>+</sup>], but not [*PrD*<sub>157</sub><sup>+</sup>], in cells expressing PrD-GFP from the *GPD* promoter cause a slight growth defect.

#### **A yeast model to monitor [Het-s]/HET-S toxicity**

Analogous to *Podospora*, expression of HET-S (and its tagged versions) caused toxicity in [*PrD*<sub>157</sub><sup>+</sup>] prion cells, but not in [*prd*<sub>157</sub><sup>-</sup>] non-prion cells (Figures 1C). In addition to the growth inhibition seen in Figure 1C, assays for viability and vital cell staining showed that the expression of HET-S in [*PrD*<sub>157</sub><sup>+</sup>] cells caused cell death. To assay viability, [*PrD*<sub>157</sub><sup>+</sup>] cells expressing HET-S in 2 % gal medium were plated on dextrose (where HET-S expression was repressed) at various time points. Cell viability decreased with increased time, suggesting that HET-S expression leads to cell death (Figure 2A). Also, cultures treated with Trypan Blue, which stains dead cells, showed a consistent increase of dead cells during HET-S expression (Figure 2B).

## **HET-S does not inhibit newly synthesized PrD<sub>157</sub> protein from joining pre-existing [PrD<sub>157</sub><sup>+</sup>] aggregates**

We tested if HET-S inhibits newly formed PrD<sub>157</sub> from joining [PrD<sub>157</sub><sup>+</sup>] aggregates thereby promoting the accumulation of toxic species composed of newly formed PrD<sub>157</sub> protein. Expression of PrD<sub>157</sub>-DsRed and HET-S (or vector control) was simultaneously turned on in [PrD<sub>157</sub><sup>+</sup>] cells constitutively expressing PrD<sub>157</sub>-GFP. Cells were examined with a fluorescent microscope after 4-6 hrs of HET-S expression when about half the cells were dead. We asked if HET-S expression inhibited newly made PrD<sub>157</sub>-DsRed from joining the pre-existing PrD<sub>157</sub>-GFP aggregates. However, no difference was detected in the appearance of PrD<sub>157</sub>-DsRed in the presence or absence of HET-S (Figure 3A). Thus, the [Het-s]/HET-S toxicity does not appear to be due to accumulation of soluble PrD<sub>157</sub>-GFP protein that was prevented from joining [PrD<sub>157</sub><sup>+</sup>] aggregates.

## **No evidence for change in [PrD<sub>157</sub><sup>+</sup>] aggregates or detergent-resistant oligomers in the presence of HET-S**

To further ask if HET-S changed non-toxic [PrD<sub>157</sub><sup>+</sup>] prion into a toxic species, we compared the sizes of [PrD<sub>157</sub><sup>+</sup>] aggregates and detergent resistant-oligomers in the presence or absence of HET-S. Gel filtration of lysates, not treated with detergent, showed the accumulation of [PrD<sub>157</sub><sup>+</sup>] in the same fractions in the presence and absence of HET-S (Figure 3B). Furthermore, the presence of HET-S did not change the size distribution of detergent resistant oligomers of [PrD<sub>157</sub><sup>+</sup>] (Figure 3C). Thus, there is no evidence for a change of [PrD<sub>157</sub><sup>+</sup>] into a toxic species.

## **HET-S aggregates in [PrD<sub>157</sub><sup>+</sup>] but not [prd<sub>157</sub><sup>-</sup>] cells**

To test if HET-S aggregates in the presence of [*PrD*<sub>157</sub><sup>+</sup>], cells were harvested following 4 hrs of HET-S expression when 50 % of the cells were dead (see Figure 2A). Lysates were subjected to high speed centrifugation and analyzed by Western blot. Both HET-S-HA and PrD<sub>157</sub>-GFP accumulated in the pellet fraction in [*PrD*<sub>157</sub><sup>+</sup>] cells, while both remained in the supernatant in [*prd*<sub>157</sub><sup>-</sup>] cells (Figure 4A). Sup35 control protein remained in the supernatant in both [*PrD*<sub>157</sub><sup>+</sup>] and [*prd*<sub>157</sub><sup>-</sup>] cells, showing that the ability of [*PrD*<sub>157</sub><sup>+</sup>] to aggregate HET-S is specific, because another yeast prion protein was unaffected. This suggests that [*PrD*<sub>157</sub><sup>+</sup>] specifically causes HET-S-HA to become insoluble. In Figure 4A, the level of total HET-S-HA and PrD<sub>157</sub>-GFP proteins in [*PrD*<sub>157</sub><sup>+</sup>] versus [*prd*<sub>157</sub><sup>-</sup>] cells is comparable. However, sometimes HET-S and PrD<sub>157</sub> protein levels are less in [*prd*<sub>157</sub><sup>-</sup>] compared to [*PrD*<sub>157</sub><sup>+</sup>] lysates even though same amounts of total protein is loaded. This occurs due to more degradation of the two proteins in non-prion lysates where they are soluble compared to the prion lysates where they are aggregated.

**In the presence of [*PrD*<sub>157</sub><sup>+</sup>], HET-S localizes near the cell periphery and forms aggregates distinct from visible [*PrD*<sub>157</sub><sup>+</sup>] aggregates**

In order to visualize HET-S aggregation, *MATα* cells expressing HET-S-DsRed, which showed diffuse fluorescence, were mated to *MATα* [*PrD*<sub>157</sub><sup>+</sup>] and [*prd*<sub>157</sub><sup>-</sup>] cells. This cell fusion experiment is directly relevant to the biological process of heterokaryon incompatibility in *Podospora*, where [Het-s]/HET-S induced cell death occurs following cell fusion.

When [*PrD*<sub>157</sub><sup>+</sup>] cells were mated with cells expressing HET-S-DsRed for 4 hours, in all the fusion cells HET-S-DsRed changed from being cytoplasmically diffuse to being

localized to the cell periphery (Figure 4B). In addition to the cell periphery localization, HET-S-DsRed punctae could also be observed in 50 % of the fused cells. Cell fusion did not appear to be complete at this time, since HET-S-DsRed and [*PrD*<sub>157</sub><sup>+</sup>] were generally each observed in opposite lobes of the fused cell and no colocalization between HET-S-DsRed and [*PrD*<sub>157</sub><sup>+</sup>] dots was observed. However, some [*PrD*<sub>157</sub><sup>+</sup>] seed that is undetectable as GFP fluorescence with the microscope must have gotten into the cell expressing HET-S-DsRed, because the HET-S only appears at the cell periphery and punctae in the presence of the prion. Such fusion cells that did not show complete cytoplasmic mixing failed to take up the vital dye, Trypan Blue. However, rare fusion cells at this time point that showed complete cytoplasmic mixing and HET-S at the entire fusion cell periphery took up the vital dye, indicating cell death.

When the fusion cells were observed after 8 hrs of mating, most fusions had undergone complete cytoplasmic mixing and HET-S-DsRed showed both cell periphery localization and punctae in ~ 70 % of fusion cells, while ~10 % and ~20 % of fusion cells showed only cell periphery localization and only HET-S-DsRed punctae respectively (Figure 4B). It is possible that the dimmer cell periphery localization could not be visualized in some cells due to the brightness of HET-S-DsRed punctae, or as the cell fusion proceeds, HET-S-DsRed at the cell periphery might aggregate into big intracellular punctae. The cell periphery localization of HET-S-DsRed appeared in all focal planes (not shown) suggesting that it assembled as a sphere along the entire periphery of the cell, distinct from ring-like aggregates that are observed for prions (39). [*PrD*<sub>157</sub><sup>+</sup>] was never observed at the cell periphery. Importantly, all 8 hr fusion cells

failed to bud and took the vital dye, Trypan Blue, thereby mimicking cell death of fusion cells in *Podospora*.

Additionally, after 8 hrs of mating, HET-S-DsRed aggregates did not colocalize with any PrD<sub>157</sub>-GFP aggregates in 84.6 % of fusion cells (52 counted), while in the remaining 15.4 % of fusions, along with independent HET-S-DsRed aggregates, some HET-S-DsRed punctae also colocalized with [PrD<sub>157</sub><sup>+</sup>] dots.

In contrast to the toxicity seen with [PrD<sub>157</sub><sup>+</sup>], when HET-S-DsRed expressing cells were fused with [prd<sub>157</sub><sup>-</sup>] cells, HET-S-DsRed remained diffuse throughout the fused cells and daughter buds appeared (Figure 4C) indicating that HET-S relocation and toxicity are specific to the interaction with the prion conformation of the HET-s PrD<sub>157</sub>.

#### **HET-S aggregation is also toxic in [PrD<sup>+</sup>]**

We tested if the prion form of Het-s PrD (218-289)-GFP is also toxic with HET-S. Like [PrD<sub>157</sub><sup>+</sup>] cells, HET-S expression in [PrD<sup>+</sup>] cells, but not [prd<sup>-</sup>] cells, caused toxicity. HET-S-HA aggregated in the pellet upon high speed centrifugation and HET-S-DsRed cell fusions to [PrD<sup>+</sup>] cells were also unable to bud and HET-S was seen along the cell periphery and as independent aggregates in addition to some localization to the [PrD<sup>+</sup>] dots (Figure 5).

#### **HET-S does not aggregate in cells dying due to another prion**

To test if HET-S aggregation was an artifact of a cell death reaction, we examined the fate of HET-S in [PSI<sup>+</sup>] cells that were dying because of overexpressed Sup35, Figure 6A (54). In such cells, HET-S-HA did not accumulate in the pellet (Figure 6B). Additionally, when [PSI<sup>+</sup>] cells were mated to cells overexpressing Sup35 and HET-S-DsRed, HET-S-DsRed did not aggregate as punctae or accumulated at the cell periphery

(Figure 6C), suggesting that HET-S aggregation and localization to cell periphery are the result of a specific interaction with [Het-s] prion forms and not just cell death.

**During heterokaryon incompatibility in *Podospora*, HET-S localizes to the cell periphery and forms aggregates distinct from visible [Het-s] aggregates**

The observations made above in yeast prompted us to look for similar events in *Podospora*. We confronted *Podospora* expressing HET-S-GFP with a [Het-s] (RFP tagged or untagged) prion strain and imaged these incompatible fusion events with fluorescence microscopy. At the fusion sites, HET-S localized to the cell periphery and also formed dots (Figure 7A). There was generally no colocalization of HET-s-RFP with HET-S-GFP at the cell periphery. In addition to finding dots with coaggregation of HET-S-GFP with HET-s-RFP, as was previously reported (28), we also found HET-S dots with no detectable HET-s-RFP fluorescence. Thus, as seen in yeast, HET-S can localize to cell periphery and form dots that are distinct from visible [Het-s] aggregates.

Formation of HET-S-GFP dots was more frequently observed in transformants showing a high level of HET-S-GFP expression and was observed in the fusion cells and in adjacent cells. Localization of the HET-S protein at the cell periphery correlated with cell death while formation of HET-S dots did not (Figure 7B). This observation was quantified: of 262 fungal articles with HET-S-GFP at the cell periphery, 261 were propidium iodine positive. Cells with HET-S-GFP fluorescence at the cell periphery were propidium iodine positive whether or not they contained dots. In contrast, of 172 cells with dots and no HET-S-GFP at the cell periphery, only 2 were propidium iodine positive. As a control for autofluorescence, an untagged *het-S* strain was also confronted

with a HET-s-RFP strain, no green fluorescence at the cell periphery was observed in this incompatible fusion.

### **HET-S binds to prion and non-prion forms of PrD<sub>157</sub>-GFP**

HET-s and HET-S proteins were shown to bind in two hybrid assays (14). We performed co-immunocapture in [*PrD<sub>157</sub><sup>+</sup>*] and [*prd<sub>157</sub><sup>-</sup>*] cells expressing HET-S-HA, and although the amount of protein expressed and obtained from the dying [*PrD<sub>157</sub><sup>+</sup>*] cells was not comparable to that in the healthy [*prd<sub>157</sub><sup>-</sup>*] cells, we detected binding of HET-S to PrD<sub>157</sub>-GFP in both the prion and non-prion forms (not shown).

### **HET-S does not form high molecular weight, prion-like oligomers**

To test if HET-S forms prion-like, detergent resistant oligomers, lysates from [*PrD<sub>157</sub><sup>+</sup>*] cells expressing HET-S-HA were treated with 2 % sarkosyl at room temperature and run on a 1.5 % agarose gel. As expected [*PrD<sub>157</sub><sup>+</sup>*] itself formed sarkosyl resistant oligomers, however similar detergent resistant high molecular weight oligomers were not detected for HET-S-HA (Figure 8A), further highlighting the difference between HET-S and [*PrD<sub>157</sub><sup>+</sup>*] aggregates.

### **HET-S aggregates break down into detergent resistant trimer-sized oligomers**

To further characterize [*PrD<sub>157</sub><sup>+</sup>*] seeded HET-S aggregates *in vivo*, we analyzed detergent treated HET-S lysates on acrylamide gels. Upon 2 % SDS treatment at room temperature, [*PrD<sub>157</sub><sup>+</sup>*] seeded HET-S-HA showed monomers (36 kDa) and SDS-resistant trimer-sized oligomers (~108 kDa) and an occasional dimer-sized (~72 kDa) HET-S-HA band (Figure 8B, left). Since the lysates were only partially denatured by the SDS treatment, the estimated molecular weights of the bands may not reflect their actual sizes. Hence we refer to these bands as apparently dimer- and trimer-sized. HET-S-HA in

[*prd<sub>157</sub>*<sup>-</sup>] cells showed only a monomer band upon SDS treatment. Importantly, the trimer-sized oligomers were not observed for PrD<sub>157</sub>-GFP (Figure 8B, middle), suggesting that PrD<sub>157</sub>-GFP is not a part of the trimer-sized complex seen for HET-S and that the HET-S conformation is different from that of [*PrD<sub>157</sub>*<sup>+</sup>].

Next we used gel filtration to determine if the HET-S trimer-sized oligomers appear in lysates of [*PrD<sub>157</sub>*<sup>+</sup>] cells without detergent treatment. HET-S-HA was concentrated in high molecular weight fractions with no HET-S appearing at the size of HET-S trimer-sized oligomers. Rather, these large HET-S aggregates only broke into monomer, dimer- and trimer-sized complexes when subjected to SDS-treatment at room temperature (Figure 8C).

**HET-S incompatibility mutants that are sequestered into [*PrD<sub>157</sub>*<sup>+</sup>] aggregates are not toxic**

The E86K mutation in the HeLo domain of HET-S leads to loss of the incompatibility function in *Podospora* (15). HET-S (E86K) can form a prion that is infectious, converting [Het-s\*] to the prion form. The infectious HET-S (E86K) is compatible with both wild type (WT) HET-S and WT HET-s. Structural studies showed that the HET-S (E86K) mutation disrupts HeLo domain dimerization and that full length HET-S (E86K) is unable to repress HET-s PrD amyloid formation *in vitro* (28).

The T266P mutation in the  $\beta$ 3b  $\beta$ -strand of the HET-s prion domain prevents prion formation in *Podospora* and yeast and drastically reduces amyloid formation *in vitro* and inclusion body formation in *E. coli* (15, 46, 53, 57). The same mutation in HET-S makes it compatible with [Het-s] in *Podospora* (28).

In yeast, expression of HET-S (E86K) or HET-S (T266P) was not toxic in  $[PrD_{157}^+]$  cells (Figure 9A). HET-S (E86K)-HA or wild type (WT) HET-S-HA were found only in the pellet when expressed in  $[PrD_{157}^+]$  cells (Figure 9B, middle row). Thus HET-S aggregation *per se* is not toxic even though HET-S (E86K), like the WT HET-S, formed SDS-resistant trimer-sized oligomers in  $[PrD_{157}^+]$  cells (Figure 9C). In contrast, HET-S (T266P)-HA expressed in  $[PrD_{157}^+]$  cells only partially accumulated in the pellet (Figure 9B) and did not show detergent resistant trimer-sized oligomers (Figure 9C).

To compare the aggregation and localization of HET-S WT and mutant proteins in the presence of  $[PrD_{157}^+]$ , cells expressing HET-S WT, E86K or T266P tagged with DsRed were mated to  $[PrD_{157}^+]$  cells. Like the WT HET-S, HET-S (E86K) changes from diffuse to aggregated when fused to  $[PrD_{157}^+]$  cells, however, unlike the WT HET-S aggregates (Figure 9D, top row), HET-S (E86K)-DsRed aggregates completely colocalized with  $[PrD_{157}^+]$  aggregates and were never observed near the cell periphery (Figure 9D, middle row). In HET-S (T266P)/ $[PrD_{157}^+]$  cell fusions, HET-S (T266P) remained mostly diffuse and the rare HET-S (T266P) foci colocalized with  $[PrD_{157}^+]$  foci (Figure 9D, bottom row). Interestingly, HET-S (T266P) appeared to interfere with  $[PrD_{157}^+]$  aggregation causing it to be more diffuse.

#### **Aggregation of HET-S mutants requires the continued presence of $[PrD_{157}^+]$**

Since HET-S (E86K) (and HET-S (T266P) partially) aggregated, but did not kill  $[PrD_{157}^+]$  cells, we asked if the mutant HET-S could remain aggregated in cells that lost the plasmid expressing PrD<sub>157</sub>-GFP and therefore lost  $[PrD_{157}^+]$ . However, centrifugation of lysates expressing mutant HET-S-HA, that lost  $[PrD_{157}^+]$ , showed that the mutant proteins were distributed evenly in supernatant and pellet fractions (Figure 9B, bottom

row) just like unseeded mutants that were never in the presence of [*PrD*<sub>157</sub><sup>+</sup>] (Figure 9B, top row). Since, HET-S WT, E86K and T266P are full length proteins, we used full length WT HET-s as a control. Indeed, WT HET-s was seeded to aggregate by [*PrD*<sub>157</sub><sup>+</sup>] and [*PrD*<sup>+</sup>] and remained aggregated even when the seed was lost (not shown). Thus, although HET-S (E86K), and to a lesser extent HET-S (T266P), can be seeded to aggregate, they do not remain in a prion form like the WT HET-s.

### **Incorporation of the HET-S HeLo domain into aggregates via heterologous prion domains does not cause toxicity**

To test if simply bringing the HET-S HeLo domains together in an aggregate is toxic, we used yeast prion forming domains to guide the incorporation of HET-S HeLo domain into aggregates. HET-S HeLo domain fused to prion domains of Sup35 (aas 1-254) (21) and Rnq1 (aas 176-405) (31, 55) were respectively expressed in [*PSI*<sup>+</sup>] or [*PIN*<sup>+</sup>] cells (or [*psi*<sup>-</sup>][*pin*<sup>-</sup>] controls) that would attract the HET-S (1-227) fusion protein into the prion aggregate. The *CUP1* promoter was used to express the fusion constructs and the expression was checked by Western blotting. Expression from both *CUP1* and *GALI* promoters has been reported to increase protein levels 10-20 fold (27). No toxicity was observed in any case although fusion proteins were confirmed to be aggregated by high speed centrifugation when expressed in the corresponding prion cells (Figure 10). Thus, the HET-S HeLo domain does not cause toxicity when drawn into any prion aggregate. Rather, toxicity requires the *bona fide* [Het-s] prion.

### **Sis1 overexpression rescues [*PrD*<sub>157</sub><sup>+</sup>]-HET-S toxicity**

We tested the chaperones, Hsp104 and Sis1, known to affect prion propagation and toxicity (11, 24, 29, 38, 40, 51, 52), for effects on [*PrD*<sub>157</sub><sup>+</sup>]/HET-S toxicity.

[*PrD<sub>157</sub><sup>+</sup>*] cells transformed with pHET-S-HA and pGal-Hsp104 or pGal-Sis1 or control vector were spotted on 2 % gal plates to simultaneously turn on HET-S-HA and chaperone expression. [*PrD<sub>157</sub><sup>+</sup>*] cells overexpressing Sis1, but not Hsp104, grew (Figure 11A).

When Sis1 was overexpressed, detergent-resistant oligomers of [*PrD<sub>157</sub><sup>+</sup>*] were not observed on agarose gels (Figure 11B) and HET-S was not seeded to aggregate. Both PrD<sub>157</sub>-GFP and HET-S-HA were found largely in the supernatant fraction when Sis1 was overexpressed, while when vector control or Hsp104 was overexpressed, PrD<sub>157</sub>-GFP and HET-S-HA remained largely aggregated in the pellet (Figure 11C). Even after Sis1 overexpression was shut down PrD<sub>157</sub>-GFP remained in the non-prion diffuse form (Figure 11D). Thus, transiently overexpressed Sis1 cures cells of [*PrD<sub>157</sub><sup>+</sup>*], thereby rescuing toxicity with HET-S. Also, neither excess Ssa1 nor excess Sse1 rescued the toxicity.

## **Discussion**

What causes amyloid and prion associated toxicity is not well understood. Sometimes amyloid toxicity is associated with the accumulation of toxic soluble oligomers of the amyloid protein (24, 26). Alternatively, proteins in their amyloid form have been shown to sequester essential factors thereby causing toxicity (12, 33, 54). In the particular case of [Het-s]/HET-S cell death, it has been proposed that the C-terminal region of HET-S is templated into the amyloid fold by [Het-s] prion seeds which induces un/refolding of the HeLo domain of HET-S into a toxic entity (28). Here, using yeast and *Podospora*, we find no evidence that [Het-s] prion related toxicity is due to the accumulation of a toxic soluble or amyloid form of HET-S/HET-s. Rather, we find that

[Het-s] promotes the aggregation of its allelic protein HET-S into toxic aggregates. We show that HET-S aggregates in dying cells are distinct from visible [Het-s] or [*PrD*<sub>157</sub><sup>+</sup>] aggregates and have a tendency to localize at the cell periphery in both *Podospora* and in yeast.

### **[Het-s]/HET-S incompatibility in yeast**

Fungal incompatibility systems trigger the death of fusion cells made from genetically distinct strains. [Het-s]/HET-S incompatibility stands out among amyloid-associated toxicity mechanisms because here amyloid-associated toxicity occurs not as a pathological mishap but as an integrated biological process. This study shows that [Het-s]/HET-S toxicity can be faithfully recapitulated in an evolutionarily remote heterologous system. Like in *Podospora*, the yeast toxicity is specifically associated with the interaction of HET-S with [*PRION*<sup>+</sup>] forms of HET-s-derived constructs. Mutations that abolish HET-S incompatibility in *Podospora* also abolish HET-S toxicity in yeast. Since [Het-s]/HET-S incompatibility can be replicated in yeast that lacks a *het-s* or any other heterokaryon incompatibility gene, it is unlikely that [Het-s]/HET-S incompatibility results from activation of a complex cell signaling cascade specific to *Podospora*. Thus, our results strongly suggest that the mechanism of HET-S toxicity is direct and universal.

### **Chaperones and [Het-s]/HET-S toxicity**

Hsp104 is required for propagation of most yeast prions (11, 20, 25, 38, 40, 43), and Sis1 or other Hsp40s are required for the propagation of some yeast prions (29, 35). Sis1 overexpression cures [*SWI*<sup>+</sup>] (30) and an artificial yeast prion (36). We report that overexpressing Sis1, but not Hsp104, rescued [*PrD*<sub>157</sub><sup>+</sup>]/HET-S toxicity because excess Sis1 cured cells of the [*PrD*<sub>157</sub><sup>+</sup>] prion. Excess Sis1 was also shown to rescue [*PIN*<sup>+</sup>]

associated toxicity due to Rnq1 overexpression resulting from the ability of Sis1 to change the location and aggregation of toxic Rnq1 (23, 24).

**Toxicity does not appear to be related to inhibition of HET-s aggregation or titration of an essential protein**

While amyloid toxicity is associated with the accumulation of soluble oligomeric species, the formation of large amyloid aggregates has been envisioned as a protective mechanism alleviating toxicity (24, 56). It has been hypothesized that HET-S might interact with the [Het-s] aggregates and inhibit further incorporation of HET-s into the amyloid prion causing the accumulation of toxic oligomeric HET-s species (13, 28). This model is supported by the observation that HET-S inhibits HET-s amyloid formation *in vitro* (28). However, we did not detect any soluble HET-s derived oligomers like those associated with toxicity of other amyloids (26, 32). Furthermore, in yeast, HET-S did not prevent the incorporation of newly formed PrD<sub>157</sub> into prion aggregates nor did we detect PrD<sub>157</sub>-GFP soluble oligomers. Thus, although we do not exclude the possibility of the accumulation of toxic soluble oligomers, we have no evidence for conversion of the PrD<sub>157</sub>-GFP prion protein into a toxic form.

In addition, our finding that dragging HET-S HeLo domains into prion aggregates via fused heterologous yeast prion domains caused the aggregation of HET-S but did not cause toxicity, suggests that HET-S HeLo domain does not sequester essential proteins.

**A form of HET-S that localizes to cell periphery, and not to [Het-s], as the toxic species**

Since the prion domain of HET-S is 97% identical to HET-s, and when separated from the globular HET-S domain it acts exactly like the HET-s prion domain (4), it seems

likely that the [Het-s] prion would cross-seed HET-S. Indeed, HET-s and HET-S co-localization into large aggregates *in vivo* was previously reported and genetic evidence suggests that HET-S needs to be able to adopt the HET-s amyloid fold in order to be functional (28). Furthermore, our finding that HET-S binds to both the prion and non-prion forms of PrD<sub>157</sub>-GFP, implies that cross-seeding and not just binding *per se* causes the toxicity.

The hypothesized [Het-s]/HET-S cross-seeding resembles the aggregation of CsgA protein, the major component of curli fibrils, which is seeded by the heterologous but similar CsgB (6). The yeast prion protein Sup35 has also been proposed to be cross-seeded into [*PSI*<sup>+</sup>] by another prion, [*PIN*<sup>+</sup>]. Once [*PSI*<sup>+</sup>] is established, it can propagate even without the cross-seed, i.e. when the gene encoding the [*PIN*<sup>+</sup>] prion protein, *RNQ1*, is deleted (10, 19, 41). Although this cannot be tested for WT HET-S, HET-S (E86K) does not remain aggregated after the [*PrD*<sub>157</sub><sup>+</sup>] seed is lost. Since the continued aggregation of HET-S requires the presence of [*PrD*<sub>157</sub><sup>+</sup>], an amount of [*PrD*<sub>157</sub><sup>+</sup>] too small to be detected microscopically could certainly remain associated with HET-S aggregates that do not co-localize with the visible [*PrD*<sub>157</sub><sup>+</sup>] foci. Indeed, although visible aggregates are hallmarks of prions, the actual prion seeds are too small to be seen using fluorescence microscopy and cannot be used to visualize cross-seeding. However, these seeds have been detected for other prions using FLIP/FRAP (18, 60).

HET-S aggregates have a conformation that is distinct from [*PrD*<sub>157</sub><sup>+</sup>]: HET-S, but not [*PrD*<sub>157</sub><sup>+</sup>], aggregates contain SDS-resistant trimer-sized components. Furthermore, the trimer-sized HET-S oligomers do not contain PrD<sub>157</sub>-GFP. However, the presence of such oligomers does not correlate with toxicity since HET-S (E86K)

abolished toxicity with  $[PrD_{157}^+]$ , but still aggregated and formed SDS-resistant trimer-sized oligomers. In yeast, HET-S (E86K) does not remain aggregated when  $[PrD_{157}^+]$  is lost, distinguishing this mutant from the WT HET-s protein. Additionally, our finding that HET-S (T266P) is not toxic and shows reduced aggregation indicates that a functional HET-S prion domain is required for HET-S aggregation and toxicity, supporting previous genetic evidence in *Podospora* (28). We propose that the T266P mutation affects the initial stage of seeding of HET-S aggregation by  $[PrD_{157}^+]$ , while the E86K mutation affects a more terminal step since aggregation and trimer-sized complex formation still occurs.

Another possibility, instead of cross-seeding, is that  $[PrD_{157}^+]$  prions enhance the aggregation of HET-S by depleting a cellular factor that normally prevents HET-S aggregation. Similar titration hypotheses have been proposed to explain the ability of  $[PIN^+]$  to promote the appearance of  $[PSI^+]$  (41) although there is no evidence for this hypothesis (42). The finding that pure full length HET-S protein fails to aggregate *in vitro* (28) implies that no proteins or factors are needed to inhibit HET-S aggregation. Furthermore, even when seeded by [Het-s] fibers, HET-S failed to aggregate *in vitro*. Apparently the non-prion HET-S domain inhibits HET-S aggregation. Indeed, HET-S also inhibits HET-s prion formation *in trans in vitro* (28). Something is clearly missing in the *in vitro* system that is needed to counteract this innate inhibition, possibly the membrane association seen *in vivo*.

The results presented here expand the earlier biochemical model that [Het-s] seeding of the HET-S prion domain region induces a toxic refolding of the overlapping globular HET-S HeLo domain (28). The altered HET-S either dissociates from the [Het-

s] seed and self-seeds HET-S monomers into toxic aggregates, or the initial [Het-s] seed remains associated, while mostly HET-S monomers are added to make toxic aggregates. Importantly, HET-S aggregation in a form that is associated with toxicity appeared at the cell periphery, and mutations that caused HET-S to be sequestered into [*PrD*<sub>157</sub><sup>+</sup>] aggregates were not toxic. Several lines of experiments show that HET-S aggregation *per se* is not the cause of cell death. HET-S does not aggregate or localize at the cell periphery in [*prd*<sub>157</sub><sup>-</sup>] cells that are dying for another reason. In addition, the finding that HET-S aggregation and cell periphery localization precedes cell death is consistent with the hypothesis HET-S aggregation and re-localization is a key factor in determining toxicity. Finally, the outcome of cell fusion during HET-S/[Het-s] incompatibility in *Podospora* is highly similar to the yeast toxicity model. HET-S is relocalized to the cell periphery and forms dots that fail to overlap with [Het-s] and only cells with HET-S localized at the cell periphery in *Podospora* are dead. Thus, our data now connects the toxic HET-S HeLo domain refolding with the localization of HET-S to the cell periphery.

### **Acknowledgements**

We thank Dr. Nava Segev (University of Illinois at Chicago) and members of the Liebman lab for ideas and comments on the manuscript. We thank Vibha Taneja for constructing some plasmids used in the study. This work was supported by National Institutes of Health (NIH) Grant GM56350 to S.W.L. The contents of this article are solely the responsibility of the authors and do not necessarily represent the official views of NIH.

## **References**

1. **Aguzzi, A., and T. O'Connor.** 2010. Protein aggregation diseases: pathogenicity and therapeutic perspectives. *Nat Rev Drug Discov* **9**:237-48.
2. **Aguzzi, A., and L. Rajendran.** 2009. The transcellular spread of cytosolic amyloids, prions, and prionoids. *Neuron* **64**:783-90.
3. **Bagriantsev, S. N., V. V. Kushnirov, and S. W. Liebman.** 2006. Analysis of amyloid aggregates using agarose gel electrophoresis. *Methods Enzymol* **412**:33-48.
4. **Balguerie, A., S. Dos Reis, B. Couлары-Salin, S. Chaignepain, M. Sabourin, J. M. Schmitter, and S. J. Saupe.** 2004. The sequences appended to the amyloid core region of the HET-s prion protein determine higher-order aggregate organization in vivo. *J Cell Sci* **117**:2599-610.
5. **Balguerie, A., S. Dos Reis, C. Ritter, S. Chaignepain, B. Couлары-Salin, V. Forge, K. Bathany, I. Lascu, J. M. Schmitter, R. Riek, and S. J. Saupe.** 2003. Domain organization and structure-function relationship of the HET-s prion protein of *Podospora anserina*. *Embo J* **22**:2071-81.
6. **Bian, Z., and S. Normark.** 1997. Nucleator function of CsgB for the assembly of adhesive surface organelles in *Escherichia coli*. *Embo J* **16**:5827-36.
7. **Boeke, J. D., J. Trueheart, G. Natsoulis, and G. R. Fink.** 1987. 5-Fluoroorotic acid as a selective agent in yeast molecular genetics. *Methods Enzymol* **154**:164-75.
8. **Brachmann, A., U. Baxa, and R. B. Wickner.** 2005. Prion generation in vitro: amyloid of Ure2p is infectious. *Embo J* **24**:3082-92.

9. **Bradley, M. E., H. K. Edskes, J. Y. Hong, R. B. Wickner, and S. W. Liebman.** 2002. Interactions among prions and prion "strains" in yeast. *Proc Natl Acad Sci U S A* **99 Suppl 4**:16392-9.
10. **Bradley, M. E., and S. W. Liebman.** 2003. Destabilizing interactions among [PSI(+)] and [PIN(+)] yeast prion variants. *Genetics* **165**:1675-85.
11. **Chernoff, Y. O., S. L. Lindquist, B. Ono, S. G. Inge-Vechtomov, and S. W. Liebman.** 1995. Role of the chaperone protein Hsp104 in propagation of the yeast prion-like factor [psi+]. *Science* **268**:880-4.
12. **Cooper, A. A., A. D. Gitler, A. Cashikar, C. M. Haynes, K. J. Hill, B. Bhullar, K. Liu, K. Xu, K. E. Strathearn, F. Liu, S. Cao, K. A. Caldwell, G. A. Caldwell, G. Marsischky, R. D. Kolodner, J. Labaer, J. C. Rochet, N. M. Bonini, and S. Lindquist.** 2006. Alpha-synuclein blocks ER-Golgi traffic and Rab1 rescues neuron loss in Parkinson's models. *Science* **313**:324-8.
13. **Coustou-Linares, V., M. L. Maddelein, J. Begueret, and S. J. Saupe.** 2001. In vivo aggregation of the HET-s prion protein of the fungus *Podospora anserina*. *Mol Microbiol* **42**:1325-35.
14. **Coustou, V., C. Deleu, S. Saupe, and J. Begueret.** 1997. The protein product of the het-s heterokaryon incompatibility gene of the fungus *Podospora anserina* behaves as a prion analog. *Proc Natl Acad Sci U S A* **94**:9773-8.
15. **Coustou, V., C. Deleu, S. J. Saupe, and J. Begueret.** 1999. Mutational analysis of the [Het-s] prion analog of *Podospora anserina*. A short N-terminal peptide allows prion propagation. *Genetics* **153**:1629-40.

16. **Cross, F. R.** 1997. 'Marker swap' plasmids: convenient tools for budding yeast molecular genetics. *Yeast* **13**:647-53.
17. **Dagkesamanskaya, A. R., and M. D. Ter-Avanesyan.** 1991. Interaction of the yeast omnipotent suppressors SUP1(SUP45) and SUP2(SUP35) with non-mendelian factors. *Genetics* **128**:513-20.
18. **Derdowski, A., S. S. Sindi, C. L. Klaips, S. DiSalvo, and T. R. Serio.** 2010. A size threshold limits prion transmission and establishes phenotypic diversity. *Science* **330**:680-3.
19. **Derkatch, I. L., M. E. Bradley, J. Y. Hong, and S. W. Liebman.** 2001. Prions affect the appearance of other prions: the story of [PIN(+)]. *Cell* **106**:171-82.
20. **Derkatch, I. L., M. E. Bradley, P. Zhou, Y. O. Chernoff, and S. W. Liebman.** 1997. Genetic and environmental factors affecting the de novo appearance of the [PSI<sup>+</sup>] prion in *Saccharomyces cerevisiae*. *Genetics* **147**:507-19.
21. **Derkatch, I. L., Y. O. Chernoff, V. V. Kushnirov, S. G. Inge-Vechtomov, and S. W. Liebman.** 1996. Genesis and variability of [PSI] prion factors in *Saccharomyces cerevisiae*. *Genetics* **144**:1375-86.
22. **Dos Reis, S., B. Coulary-Salin, V. Forge, I. Lascu, J. Begueret, and S. J. Saupe.** 2002. The HET-s prion protein of the filamentous fungus *Podospora anserina* aggregates in vitro into amyloid-like fibrils. *J Biol Chem* **277**:5703-6.
23. **Douglas, P. M., D. W. Summers, H. Y. Ren, and D. M. Cyr.** 2009. Reciprocal efficiency of RNQ1 and polyglutamine detoxification in the cytosol and nucleus. *Mol Biol Cell* **20**:4162-73.

24. **Douglas, P. M., S. Treusch, H. Y. Ren, R. Halfmann, M. L. Duennwald, S. Lindquist, and D. M. Cyr.** 2008. Chaperone-dependent amyloid assembly protects cells from prion toxicity. *Proc Natl Acad Sci U S A* **105**:7206-11.
25. **Du, Z., K. W. Park, H. Yu, Q. Fan, and L. Li.** 2008. Newly identified prion linked to the chromatin-remodeling factor Swi1 in *Saccharomyces cerevisiae*. *Nat Genet* **40**:460-5.
26. **Glabe, C. G.** 2006. Common mechanisms of amyloid oligomer pathogenesis in degenerative disease. *Neurobiol Aging* **27**:570-5.
27. **Greene, J. J., and V. B. Rao.** 1998. Recombinant DNA principles and methodologies. Marcel Dekker Inc, New York.
28. **Greenwald, J., C. Buhtz, C. Ritter, W. Kwiatkowski, S. Choe, M. L. Maddelein, F. Ness, S. Cescau, A. Soragni, D. Leitz, S. J. Saupe, and R. Riek.** 2010. The mechanism of prion inhibition by HET-S. *Mol Cell* **38**:889-99.
29. **Higurashi, T., J. K. Hines, C. Sahi, R. Aron, and E. A. Craig.** 2008. Specificity of the J-protein Sis1 in the propagation of 3 yeast prions. *Proc Natl Acad Sci U S A* **105**:16596-601.
30. **Hines, J. K., X. Li, Z. Du, T. Higurashi, L. Li, and E. A. Craig.** 2011. [SWI], the prion formed by the chromatin remodeling factor Swi1, is highly sensitive to alterations in Hsp70 chaperone system activity. *PLoS Genet* **7**:e1001309.
31. **Kadnar, M. L., G. Articov, and I. L. Derkatch.** 2010. Distinct type of transmission barrier revealed by study of multiple prion determinants of Rnq1. *PLoS Genet* **6**:e1000824.

32. **Kayed, R., E. Head, J. L. Thompson, T. M. McIntire, S. C. Milton, C. W. Cotman, and C. G. Glabe.** 2003. Common structure of soluble amyloid oligomers implies common mechanism of pathogenesis. *Science* **300**:486-9.
33. **Kim, S., E. A. Nollen, K. Kitagawa, V. P. Bindokas, and R. I. Morimoto.** 2002. Polyglutamine protein aggregates are dynamic. *Nat Cell Biol* **4**:826-31.
34. **King, C. Y., and R. Diaz-Avalos.** 2004. Protein-only transmission of three yeast prion strains. *Nature* **428**:319-23.
35. **Kirkland, P. A., M. Reidy, and D. C. Masison.** 2011. Functions of yeast Hsp40 chaperone Sis1p dispensable for prion propagation but important for prion curing and protection from prion toxicity. *Genetics* **188**:565-77.
36. **Kryndushkin, D. S., V. N. Smirnov, M. D. Ter-Avanesyan, and V. V. Kushnirov.** 2002. Increased expression of Hsp40 chaperones, transcriptional factors, and ribosomal protein Rpp0 can cure yeast prions. *J Biol Chem* **277**:23702-8.
37. **Maddelein, M. L., S. Dos Reis, S. Duvezin-Caubet, B. Couлары-Salin, and S. J. Saupe.** 2002. Amyloid aggregates of the HET-s prion protein are infectious. *Proc Natl Acad Sci U S A* **99**:7402-7.
38. **Malato, L., S. Dos Reis, L. Benkemoun, R. Sabate, and S. J. Saupe.** 2007. Role of Hsp104 in the Propagation and Inheritance of the [Het-s] Prion. *Mol Biol Cell* **18**:4803-12.
39. **Mathur, V., V. Taneja, Y. Sun, and S. W. Liebman.** 2010. Analyzing the birth and propagation of two distinct prions, [PSI<sup>+</sup>] and [Het-s](y), in yeast. *Mol Biol Cell* **21**:1449-61.

40. **Moriyama, H., H. K. Edskes, and R. B. Wickner.** 2000. [URE3] prion propagation in *Saccharomyces cerevisiae*: requirement for chaperone Hsp104 and curing by overexpressed chaperone Ydj1p. *Mol Cell Biol* **20**:8916-22.
41. **Osherovich, L. Z., and J. S. Weissman.** 2001. Multiple Gln/Asn-rich prion domains confer susceptibility to induction of the yeast [PSI(+)] prion. *Cell* **106**:183-94.
42. **Osherovich, L. Z., and J. S. Weissman.** 2002. The utility of prions. *Dev Cell* **2**:143-51.
43. **Patel, B. K., J. Gavin-Smyth, and S. W. Liebman.** 2009. The yeast global transcriptional co-repressor protein Cyc8 can propagate as a prion. *Nat Cell Biol.*
44. **Patel, B. K., and S. W. Liebman.** 2007. "Prion-proof" for [PIN+]: infection with in vitro-made amyloid aggregates of Rnq1p-(132-405) induces [PIN+]. *J Mol Biol* **365**:773-82.
45. **Prusiner, S. B.** 1998. Prions. *Proc Natl Acad Sci U S A* **95**:13363-83.
46. **Ritter, C., M. L. Maddelein, A. B. Siemer, T. Luhrs, M. Ernst, B. H. Meier, S. J. Saupe, and R. Riek.** 2005. Correlation of structural elements and infectivity of the HET-s prion. *Nature* **435**:844-8.
47. **Saupe, S. J.** 2000. Molecular genetics of heterokaryon incompatibility in filamentous ascomycetes. *Microbiol Mol Biol Rev* **64**:489-502.
48. **Saupe, S. J., C. Clave, and J. Begueret.** 2000. Vegetative incompatibility in filamentous fungi: *Podospora* and *Neurospora* provide some clues. *Curr Opin Microbiol* **3**:608-12.

49. **Schirmer, E. C., O. R. Homann, A. S. Kowal, and S. Lindquist.** 2004. Dominant gain-of-function mutations in Hsp104p reveal crucial roles for the middle region. *Mol Biol Cell* **15**:2061-72.
50. **Sherman, F., G. R. Fink, and J. B. Hicks.** 1986. *Methods in Yeast Genetics*. Cold Spring Harbor Lab., Plainview, New York.
51. **Shorter, J., and S. Lindquist.** 2004. Hsp104 catalyzes formation and elimination of self-replicating Sup35 prion conformers. *Science* **304**:1793-7.
52. **Sondheimer N, L. N., Craig EA, Lindquist S.** 2001. The role of Sis1 in the maintenance of the [RNQ+] prion. *EMBO J.* **20**:2435-42.
53. **Taneja, V., M. L. Maddelein, N. Talarek, S. J. Saupe, and S. W. Liebman.** 2007. A non-Q/N-rich prion domain of a foreign prion, [Het-s], can propagate as a prion in yeast. *Mol Cell* **27**:67-77.
54. **Vishveshwara, N., M. E. Bradley, and S. W. Liebman.** 2009. Sequestration of essential proteins causes prion associated toxicity in yeast. *Mol Microbiol* **73**:1101-14.
55. **Vitrenko, Y. A., M. E. Pavon, S. I. Stone, and S. W. Liebman.** 2007. Propagation of the [PIN+] prion by fragments of Rnq1 fused to GFP. *Curr Genet* **51**:309-19.
56. **Wang, Y., A. B. Meriin, N. Zaarur, N. V. Romanova, Y. O. Chernoff, C. E. Costello, and M. Y. Sherman.** 2009. Abnormal proteins can form aggresome in yeast: aggresome-targeting signals and components of the machinery. *Faseb J* **23**:451-63.

57. **Wasmer, C., A. Lange, H. Van Melckebeke, A. B. Siemer, R. Riek, and B. H. Meier.** 2008. Amyloid fibrils of the HET-s(218-289) prion form a beta solenoid with a triangular hydrophobic core. *Science* **319**:1523-6.
58. **Wickner, R. B., D. C. Masison, and H. K. Edskes.** 1995. [PSI] and [URE3] as yeast prions. *Yeast* **11**:1671-85.
59. **Wickner, R. B., K. L. Taylor, H. K. Edskes, M. L. Maddelein, H. Moriyama, and B. T. Roberts.** 2000. Prions of yeast as heritable amyloidoses. *J Struct Biol* **130**:310-22.
60. **Wu, Y. X., D. C. Masison, E. Eisenberg, and L. E. Greene.** 2006. Application of photobleaching for measuring diffusion of prion proteins in cytosol of yeast cells. *Methods* **39**:43-9.

**Table 1.** Plasmids used in this study.

| Plasmid | Plasmid name                 | Description   | Reference  |
|---------|------------------------------|---|------------|
| p1389   | pGPD-HET-sPrD                | $P_{GPD}$ -HET-sPrD, URA3, <i>leu2d</i> , 2 $\mu$             | This study |
| p1587   | pGPD-PrD <sub>157</sub> -GFP | $P_{GPD}$ -HET-s PrD <sub>157</sub> -GFP, URA3                | This study |
| p1587H  | pGPD-PrD <sub>157</sub> -GFP | $P_{GPD}$ -HET-s PrD <sub>157</sub> -GFP, HIS3                | This study |
| p1902   | pPrD <sub>157</sub> -DsRed   | $P_{GPD}$ -HET-s PrD <sub>157</sub> -DsRed, URA3              | This study |
| p1566   | pHET-S                       | $P_{GALI}$ -HET-S, TRP1, CEN                                  | This study |
| p1387   | pHET-s                       | $P_{GPD}$ -HET-s, URA3, <i>leu2d</i> , 2 $\mu$                | This study |
| p1920   | pGPD-PrD-GFP                 | $P_{GPD}$ -HET-sPrD-GFP, URA3, CEN                            | This study |
| p1841   | pHET-S-HA                    | $P_{GALI}$ -HET-S-HA, TRP1, CEN                               | This study |
| p1842   | pHET-S-DsRed                 | $P_{GALI}$ -HET-S-DsRed, URA3, <i>leu2d</i> , 2 $\mu$         | This study |
| p1692   | pDsRed                       | $P_{GALI}$ -DsRed, URA3, <i>leu2d</i> , 2 $\mu$               | This study |
| p1285   | pGal-Hsp104                  | $P_{GALI}$ -HSP104, URA3                                      | (49)       |
| p1759   | pGal-Sis1                    | $P_{GALI}$ -SIS1, URA3  | (24)       |
| p1849   | pNM-S (1-227)                | $P_{CUP1}$ -SUP35NM-HET-S (1-227), URA3, CEN                  | This study |
| p1846   | pS(1-227)-Rnq1               | $P_{CUP1}$ -HET-S (1-227)-RNQ1 (172-405), HIS3, CEN           | This study |
| p1851   | pNM-s (1-227)                | $P_{CUP1}$ -SUP35NM-HET-s(1-227), URA3, CEN                   | This study |
| p1847   | ps(1-227)-Rnq1               | $P_{CUP1}$ -HET-s(1-227)-RNQ1(172-405), HIS3, CEN             | This study |
| p1880   | pE86K-HA                     | $P_{GALI}$ -HET-S (E86K)-HA, TRP1, CEN                        | This study |
| p1883   | pT266P-HA                    | $P_{GALI}$ -HET-S (T266P)-HA, TRP1, CEN                       | This study |
| p1884   | pE86K-DsRed                  | $P_{GALI}$ -HET-S (E86K)-DsRed, URA3, <i>leu2d</i> , 2 $\mu$  | This study |
| p1886   | pT266P-DsRed                 | $P_{GALI}$ -HET-S (T266P)-DsRed, URA3, <i>leu2d</i> , 2 $\mu$ | This study |
| p1760   | pSup35-GFP                   | $P_{GALI}$ -SUP35-GFP, HIS3, CEN                              | (54)       |

## **Figure legends**

**Figure 1. Yeast system to monitor [Het-s]-HET-S toxicity.** A. Domains of HET-s (white) and HET-S (gray) proteins. Prion formation and toxicity, in *Podospora* and yeast, of N-terminal HeLo domains, C-terminal prion domains (PrD and PrD<sub>157</sub>), mutants (E86K and T266P) and hybrid proteins (HET-s HeLo-HET-S PrD: white-gray, HET-S HeLo-HET-s PrD: gray-white) are depicted. B. Construction of [PrD<sub>157</sub><sup>+</sup>]. Cells (L1749) were co-transformed with pGPD-PrD<sub>157</sub>-GFP (p1587H) and pGPD-PrD (p1389). Cell with dots were micromanipulated and [PrD<sub>157</sub><sup>+</sup>] cells lacking [PrD<sup>+</sup>] were obtained by losing pGPD-PrD plasmid on 5-FOA plates. An intermediate [PrD<sub>157</sub><sup>+</sup>] stage with lines and dots is seen upon initial prion appearance. Later, [PrD<sub>157</sub><sup>+</sup>] propagated as single or multiple dots per cell. C. HET-S expression in [PrD<sub>157</sub><sup>+</sup>], but not [prd<sub>157</sub><sup>-</sup>], causes lethality. pHET-S-DsRed (or DsRed control vector), pHET-S-HA, untagged pHET-S and vector control (all under *GALI* promoter) were transformed into [PrD<sub>157</sub><sup>+</sup>] and [prd<sub>157</sub><sup>-</sup>]. Three independent transformants (one shown here) were serially diluted and spotted on 2 % gal to express HET-S or control dextrose. Spots show growth after 3 days.

**Figure 2. HET-S expression in [PrD<sub>157</sub><sup>+</sup>] cells leads to cell death.** A. [PrD<sub>157</sub><sup>+</sup>] or [prd<sub>157</sub><sup>-</sup>] cells with pHET-S-HA (p1841) were grown in liquid synthetic dextrose media to late log phase, washed and transferred to 2 % gal media at the same concentration of cells to express HET-S-HA. Samples were taken at 0, 2, 4, 6, 8 hrs and plated on synthetic dextrose plates. Colonies were counted after growth and colony forming units (CFU)/ml was calculated. The few colonies that grew at 8 hrs had lost the [PrD<sub>157</sub><sup>+</sup>] prion. B. Trypan blue staining of [PrD<sub>157</sub><sup>+</sup>] and [prd<sub>157</sub><sup>-</sup>] cells expressing HET-S-HA for the times

indicated. Cells at each time point were treated with 0.2 % Trypan Blue for 15 mins and observed with light microscopy.

**Figure 3. HET-S does not alter the properties of the [*PrD*<sub>157</sub><sup>+</sup>] prion.** A. Newly formed PrD<sub>157</sub>-DsRed efficiently joins pre-existing [*PrD*<sub>157</sub><sup>+</sup>] aggregates in the presence of HET-S. Expression of pGal-PrD<sub>157</sub>-DsRed and pGal-HET-S (p1566), or vector, was turned on by growth in 2 % gal for 4-6 hrs in [*PrD*<sub>157</sub><sup>+</sup>] cells continuously expressing PrD<sub>157</sub>-GFP. PrD<sub>157</sub>-DsRed colocalizes with PrD<sub>157</sub>-GFP in the presence of HET-S (upper panels) and vector control (bottom panels). Layers 1 and 2 depict two different focal planes of the same field showing multiple foci of [*PrD*<sub>157</sub><sup>+</sup>]. Quantification of background red fluorescent signal (indicating levels of soluble PrD<sub>157</sub>-DsRed) in cells with or without HET-S expression showed no significant difference. B. Expression of HET-S in [*PrD*<sub>157</sub><sup>+</sup>] cells does not cause the appearance of soluble PrD<sub>157</sub> oligomers. [*PrD*<sub>157</sub><sup>+</sup>] lysates expressing HET-S or vector were analyzed by gel filtration through Superose 6.0 column. C. [*PrD*<sub>157</sub><sup>+</sup>] oligomer size does not change in the presence of HET-S. pGal-HET-S (p1566) or vector was expressed in [*PrD*<sub>157</sub><sup>+</sup>] cells. Lysates treated with 2 % sarkosyl were analyzed by SDD-AGE.

**Figure 4. HET-S aggregates in [*PrD*<sub>157</sub><sup>+</sup>], but not [*prd*<sub>157</sub><sup>-</sup>] cells.** A. HET-S-HA accumulates in the pellet. High speed centrifugation of [*PrD*<sub>157</sub><sup>+</sup>] and [*prd*<sub>157</sub><sup>-</sup>] cell lysates expressing HET-S-HA (from p1841), total (T), supernatant (S) and pellet (P) were analyzed by SDS-PAGE and Western blotting. B. HET-S forms independent aggregates in [*PrD*<sub>157</sub><sup>+</sup>] cells. Shown are fusion/zygotes of HET-S-DsRed expressing cells (GF727)

mated with [*PrD*<sub>157</sub><sup>+</sup>] cells for 4 hrs (top panels) and 8hrs (bottom panels). The fusion cells failed to bud and accumulated HET-S-DsRed along the cell periphery or as punctae or both. The graph shows quantification of the HET-S-DsRed phenotypes after 8 hrs of mating. C. HET-S remains diffuse in [*prd*<sub>157</sub><sup>-</sup>] cells. Fusions of HET-S-DsRed expressing cells to [*prd*<sub>157</sub><sup>-</sup>] cells gave rise to buds and showed diffuse fluorescence. At least 30 zygotes each were observed in 3 independent experiments.

**Figure 5. HET-S aggregates and is toxic in [*PrD*<sup>+</sup>] cells.** A. HET-S is toxic in [*PrD*<sup>+</sup>] cells. Serial dilutions of [*PrD*<sup>+</sup>] and [*prd*<sup>-</sup>] cells expressing HET-S-HA and dextrose controls. B. HET-S aggregates in [*PrD*<sup>+</sup>], but not [*prd*<sup>-</sup>], cells. High speed centrifugation analysis of [*PrD*<sup>+</sup>] and [*prd*<sup>-</sup>] lysates expressing HET-S-HA. Coomassie control indicated higher protein loading of [*prd*<sup>-</sup>] vs [*PrD*<sup>+</sup>] lysates. C. HET-S forms SDS-resistant trimer-sized oligomers in [*PrD*<sup>+</sup>], but not [*prd*<sup>-</sup>], cells. [*PrD*<sup>+</sup>] and [*prd*<sup>-</sup>] lysates expressing HET-S-HA were treated with 2 % SDS and analyzed by SDS-PAGE and Western blotting. D. HET-S-DsRed localizes at the cell periphery and forms punctae when mated to [*PrD*<sup>+</sup>] cells. Cells expressing HET-S-DsRed were mated to [*PrD*<sup>+</sup>] cells and visualized after 8 hrs.

**Figure 6. HET-S does not aggregate in [*PSI*<sup>+</sup>] cells overexpressing Sup35.** A. Overexpression of pGal-Sup35-GFP causes growth inhibition in [*PSI*<sup>+</sup>], but not [*psi*<sup>-</sup>], cells. [*PSI*<sup>+</sup>] and [*psi*<sup>-</sup>] transformants containing pSup35-GFP and pHET-S-HA were serially diluted and spotted on 2 % gal or dextrose control. B. HET-S-HA does not accumulate in the pellet in dying [*PSI*<sup>+</sup>] cells overexpressing Sup35. High speed

centrifugation of [*PSI*<sup>+</sup>] and [*psi*<sup>-</sup>] lysates expressing HET-S-HA and Sup35-GFP. C. HET-S-DsRed does not localize at the cell periphery in [*PSI*<sup>+</sup>] cells dying due to excess Sup35. [*PSI*<sup>+</sup>] (top) or [*psi*<sup>-</sup>] (bottom) cells were mated to cells expressing Sup35-GFP and HET-S-DsRed and visualized after 8 hrs.

**Figure 7. HET-S-GFP localizes at the cell periphery and forms dots in incompatible cell fusions in *Podospora*.** Strains expressing HET-S-GFP and HET-s-RFP were confronted on solid medium. A. [Het-s]/HET-S confrontation zones. Outlines of the [Het-s] and HET-S filaments are drawn in red and green respectively, scale bar 4μ. Arrowheads indicate HET-S-GFP at the cell periphery. B. HET-S-GFP localization at the cell periphery, but not HET-S-GFP dot formation, is correlated with cell death. HET-S-GFP/HET-s-RFP confrontation zones were stained with either propidium iodine (left) or Evans blue (right). Cells showing HET-S-GFP localization at the cell periphery take up the vital dyes but cells containing HET-S-GFP dots (right) but showing no localization at the cell periphery do not, scale bar is 10μ. Two different vital dyes were used in order to increase confidence staining specificity. Both gave identical results.

**Figure 8. HET-S forms detergent-resistant low n-oligomers.** A. HET-S-HA does not form high molecular weight oligomers. Lysates expressing HET-S-HA in [*PrD*<sub>157</sub><sup>+</sup>] and [*prd*<sub>157</sub><sup>-</sup>] cells were treated with 2 % sarkosyl at room temperature, run on a 1.5 % agarose gel and analyzed with HA and GFP antibodies by Western blotting. B. HET-S, but not PrD<sub>157</sub>-GFP, forms SDS-resistant trimer-sized oligomers in [*PrD*<sub>157</sub><sup>+</sup>] cells. Lysates made from HET-S-HA expressing [*PrD*<sub>157</sub><sup>+</sup>] and [*prd*<sub>157</sub><sup>-</sup>] cells were treated with 2 % SDS at

room temperature and analyzed by SDS-PAGE and Western blotting. HET-S-HA (left), but not PrD<sub>157</sub>-GFP (middle), formed SDS-resistant trimer (~108 kDa) and dimer-sized (~72 kDa) oligomers in [*PrD*<sub>157</sub><sup>+</sup>] but not [*prd*<sub>157</sub><sup>-</sup>] cells. Coomassie stain ensured equal protein loading. Note: PrD<sub>157</sub>-GFP is rapidly degraded in lysates when in the non-prion form. C. HET-S aggregates break down into SDS-resistant trimer-sized oligomers. Cell lysates expressing HET-S-HA in [*PrD*<sub>157</sub><sup>+</sup>] were subjected to HPLC on a Superose 6.0 gel filtration column. Concentrated fractions were treated with 2 % SDS at room temperature and analyzed by SDS-PAGE and Western blotting. \* shows non-specific bands present in controls not expressing HET-S-HA.

**Figure 9. Non-toxic HET-S mutants do not form independent aggregates.** A. HET-S E86K and T266P are not toxic in [*PrD*<sub>157</sub><sup>+</sup>] cells. Serial dilutions of [*PrD*<sub>157</sub><sup>+</sup>] and [*prd*<sub>157</sub><sup>-</sup>] cells expressing pHET-S-HA (p1841) wild type (WT) or mutants pE86K-HA (p1880) and pT266P-HA (p1883) on 2 % gal media. B. Solubility of WT and mutant HET-S. High speed centrifugation of [*PrD*<sub>157</sub><sup>+</sup>] lysates containing WT or mutant HET-S shows total (T), supernatant (S) and pellet (P) fractions. Top row: unseeded WT and mutant HET-S proteins, middle row: [*PrD*<sub>157</sub><sup>+</sup>] seeded WT and mutant HET-S proteins, bottom row: HET-S mutants after losing [*PrD*<sub>157</sub><sup>+</sup>] (by losing pGPD-PrD<sub>157</sub>-GFP, p1587H). C. HET-S E86K, but not T266P, forms SDS-resistant trimer-sized oligomers. [*PrD*<sub>157</sub><sup>+</sup>] lysates expressing HET-S-HA WT, E86K or T266P were treated with 2 % SDS at room temperature and analyzed by Western blotting with HA antibody. \*Non-specific bands also seen in [*PrD*<sub>157</sub><sup>+</sup>] cells not expressing HET-S-HA in this experiment. D. HET-S (E86K) and HET-S (T266P) do not localize at the cell periphery, but completely

colocalize with [*PrD*<sub>157</sub><sup>+</sup>] aggregates. [*PrD*<sub>157</sub><sup>+</sup>] cells with fluorescent PrD<sub>157</sub>-GFP punctae were mated for 8 hrs with cells expressing either WT or mutant HET-S-DsRed (in L1753) which showed only diffuse fluorescence. Representative fusion cells show localization of HET-S WT (top row), HET-S (E86K) (middle row) and HET-S (T266P) (bottom row) in the presence of [*PrD*<sub>157</sub><sup>+</sup>].

**Figure 10. Fusions of the HET-S HeLo domain to heterologous prion domains**

**aggregate but do not cause toxicity.** A. Sup35NM fused to HET-S (1-227) is not toxic in [*PSI*<sup>+</sup>]. The globular non-prion domain aas 1-227 of HET-S or HET-s (control) was fused to Sup35NM domains. The Sup35NM fusions and NM-GFP controls were expressed using the *CUP1* promoter in [*PSI*<sup>+</sup>][*pin*<sup>-</sup>] (L1763) and [*psi*<sup>-</sup>][*pin*<sup>-</sup>] (L2910) cells on plasmid selective plates with 50μM Cu<sup>2+</sup>. Western blots show that the fusion proteins detected with anti-Sup35N antibody accumulate in the pellet (P) in [*PSI*<sup>+</sup>] cells. The WT Sup35 protein band (~75 kDa) is not shown in the figure. B. HET-S (1-227) fused to Rnq1 (172-405) is not toxic in [*PIN*<sup>+</sup>]. HET-S (1-227) or HET-s (1-227) were fused to Rnq1 (aas 172-405) which can propagate as a prion. These Rnq1 fusions and Rnq1 (aas 172-405) controls were expressed in [*psi*<sup>-</sup>][*PIN*<sup>+</sup>] (L1749) and [*psi*<sup>-</sup>][*pin*<sup>-</sup>] (L2910) cells on plasmid selective plates with 50μM Cu<sup>2+</sup>. Western blots show that the fusion proteins detected with anti-Rnq1 antibody accumulate in the pellet (P) in [*PIN*<sup>+</sup>] cells. The WT Rnq1 protein band (~45 kDa) is not shown in the figure. The molecular weights (kDa) of the fusion proteins are shown and they ran at their expected sizes.

**Figure 11. Sis1, but not Hsp104, overexpression rescues  $[PrD_{157}^+]$ -HET-S toxicity by curing  $[PrD_{157}^+]$ .** A. Sis1 overexpression rescues toxicity. Serial dilutions of  $[PrD_{157}^+]$  cells containing pHET-S-HA (p1841) and pGal-Hsp104 (p1285), pGal-Sis1 (p1759) or empty vector on 2 % gal media. B. Sis1 overexpression cures  $[PrD_{157}^+]$ . SDD-AGE of  $[PrD_{157}^+]$  lysates expressing either vector or Hsp104 or Sis1, in the presence of HET-S treated with 2 % sarkosyl at room temperature. C. Sis1 overexpression prevents seeding of HET-S. High speed centrifugation of  $[PrD_{157}^+]$  lysates expressing HET-S-HA along with excess Hsp104, Sis1 or vector control shows total (T), supernatant (S) and pellet (P) fractions. A portion of Coomassie stained blot shows equal loading of the total protein. The HET-S-HA and PrD<sub>157</sub>-GFP protein levels appear to be less in the Sis1 lanes since they degrade rapidly in the lysates when in the non-aggregated forms. D. Transient overexpression of Sis1 cures  $[PrD_{157}^+]$ .  $[PrD_{157}^+]$  cells showed dot aggregates (left). Upon Sis1 overexpression on 2 % gal,  $[PrD_{157}^+]$  became diffuse (middle) and remained diffuse even after Sis1 overexpression was stopped for 3 passes on dextrose (right).

Figure 1

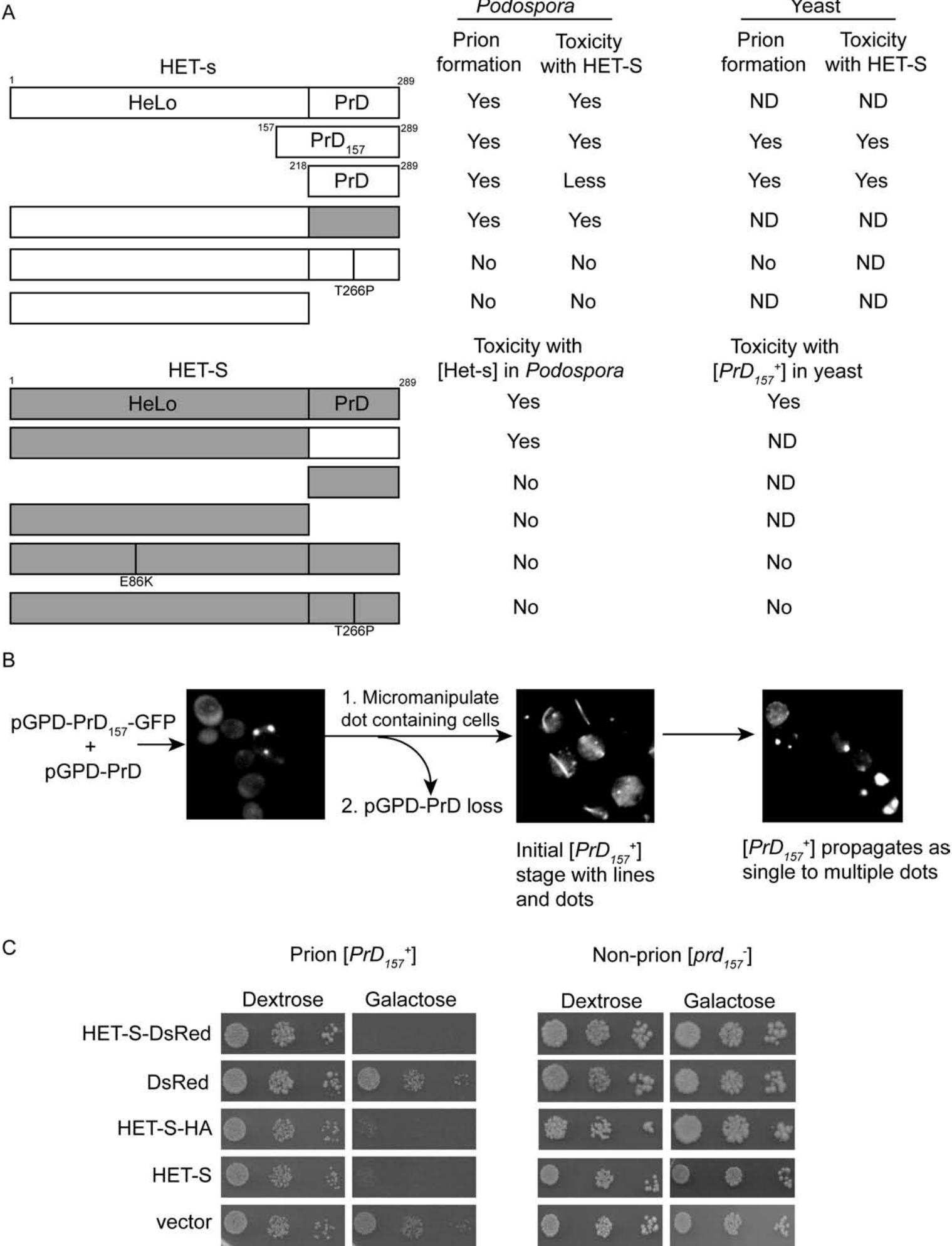
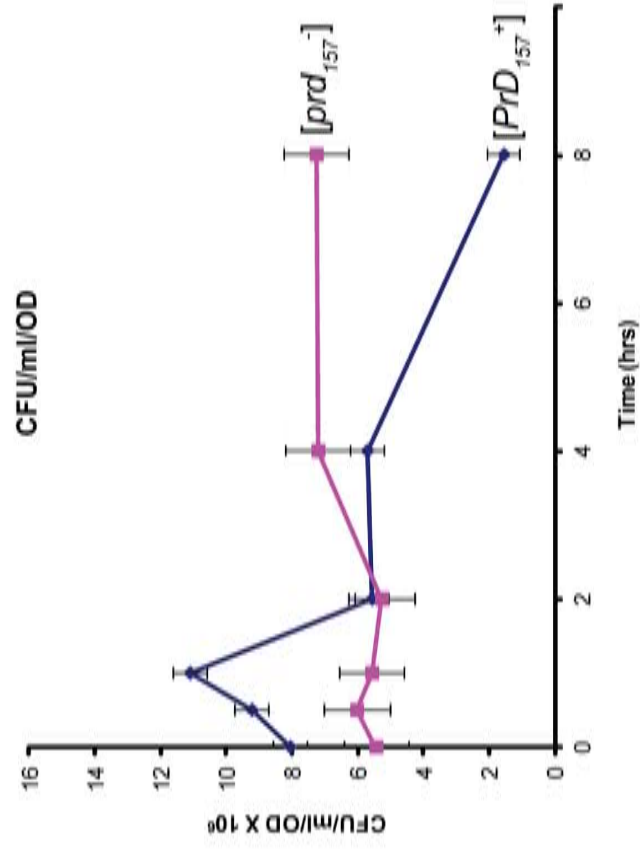


Figure 2

A



B

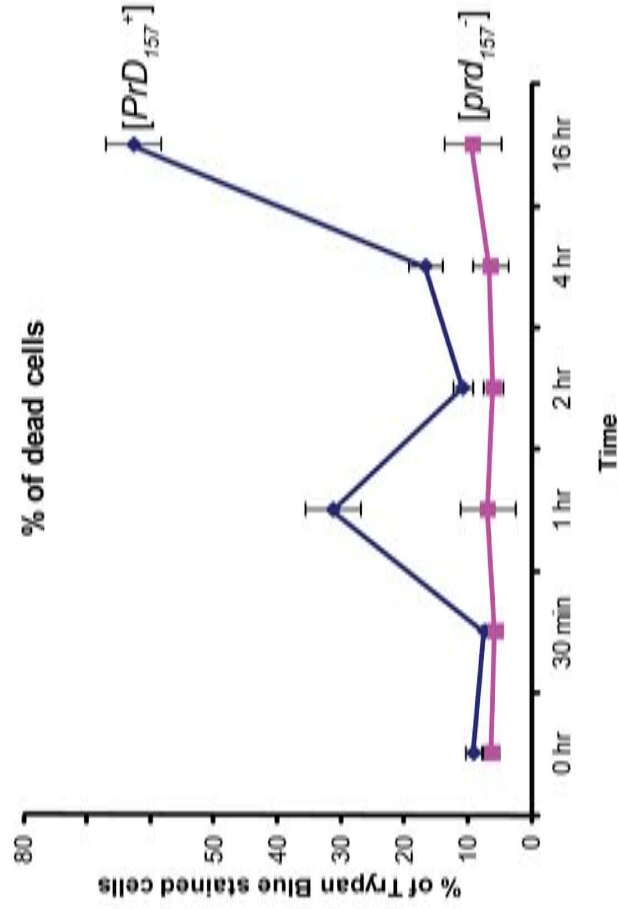


Figure 3

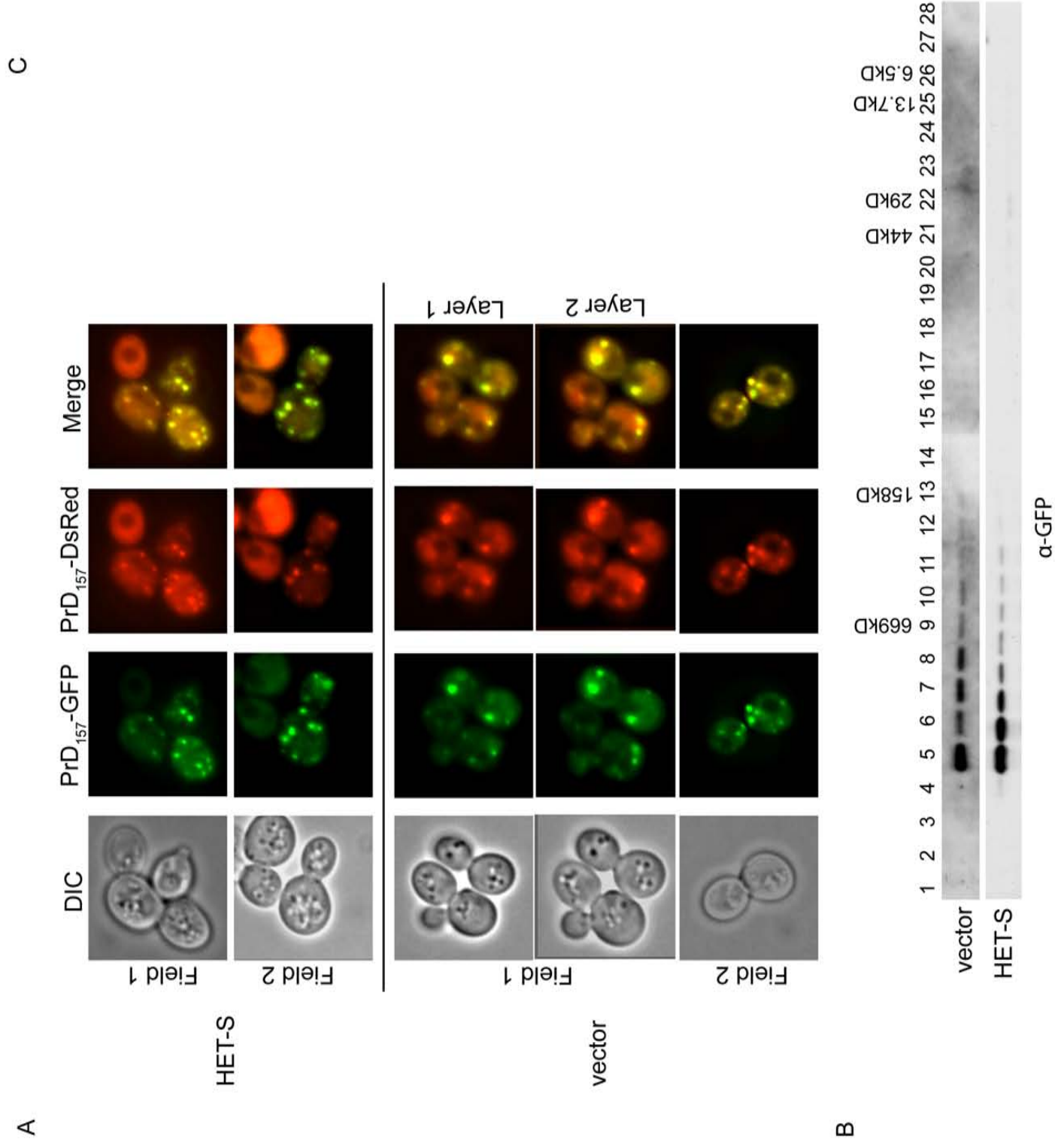
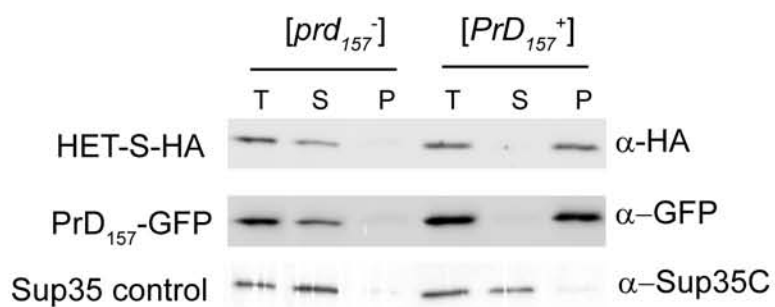
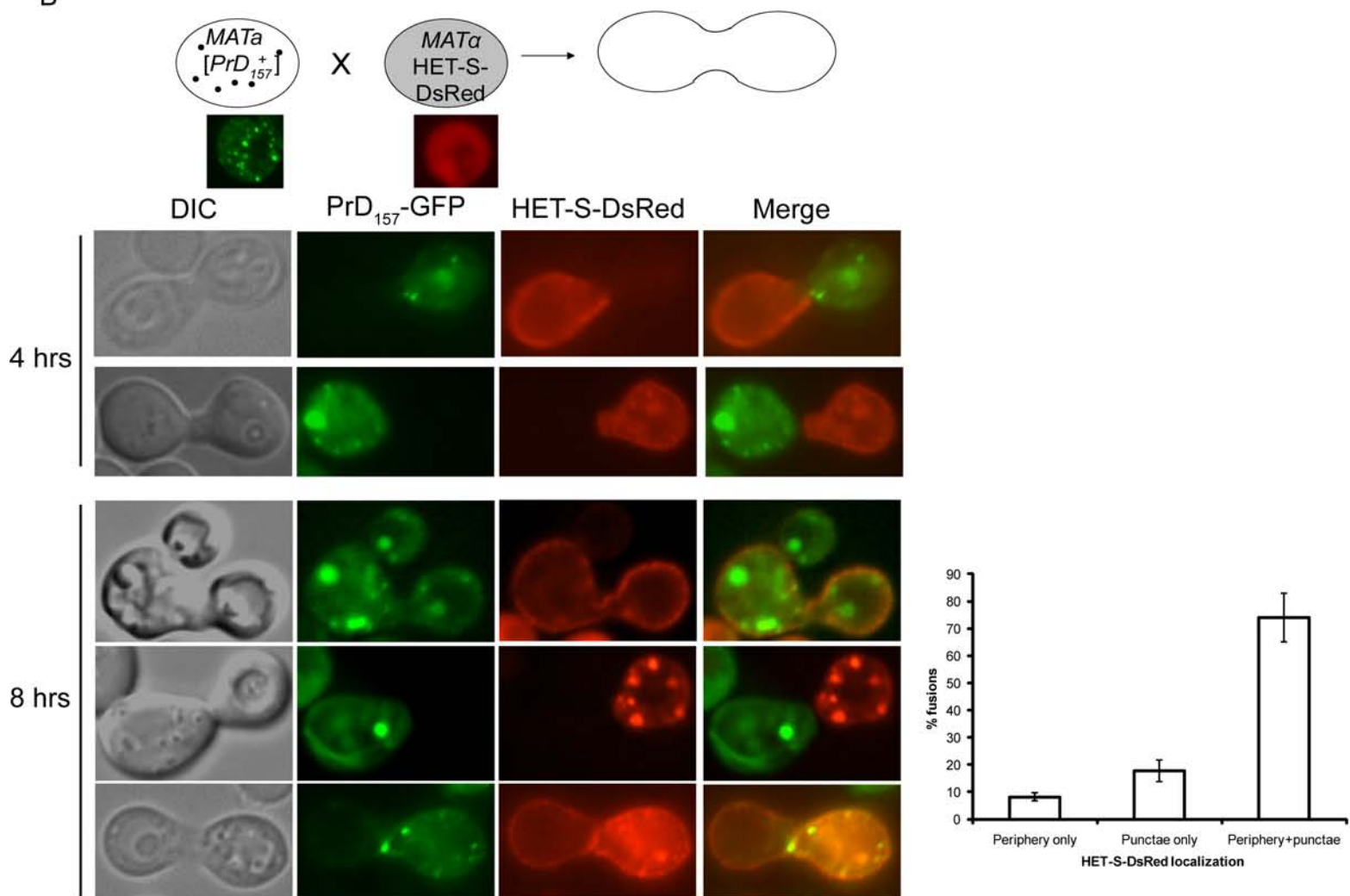


Figure 4

A



B



C

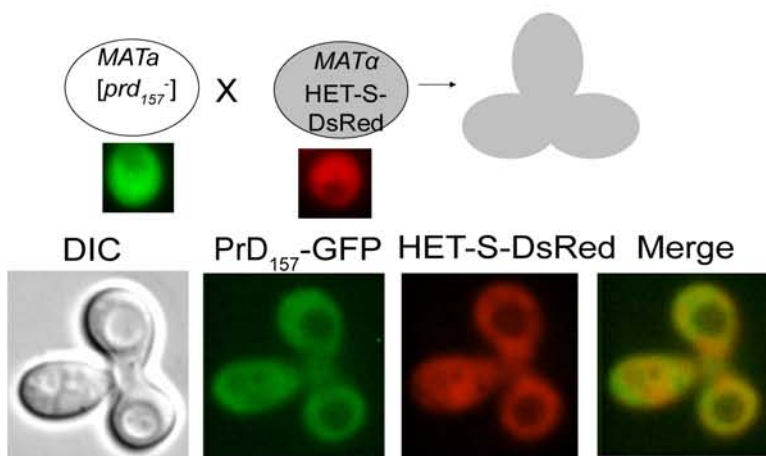
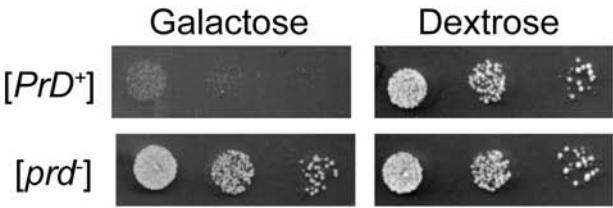
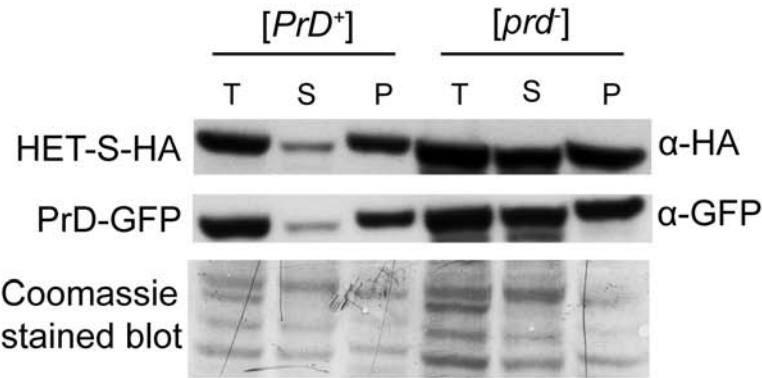


Figure 5

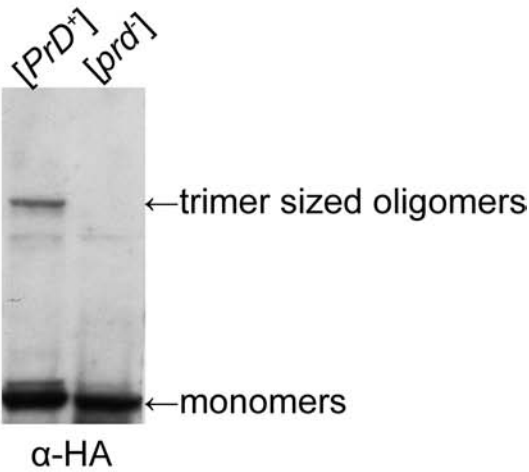
A



B



C



D

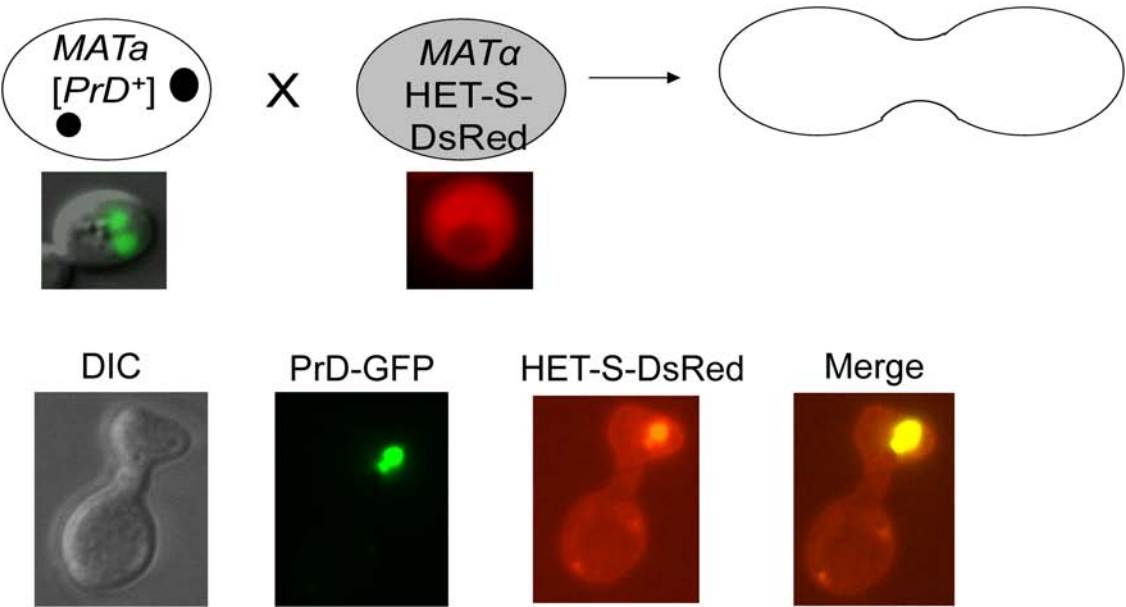


Figure 6

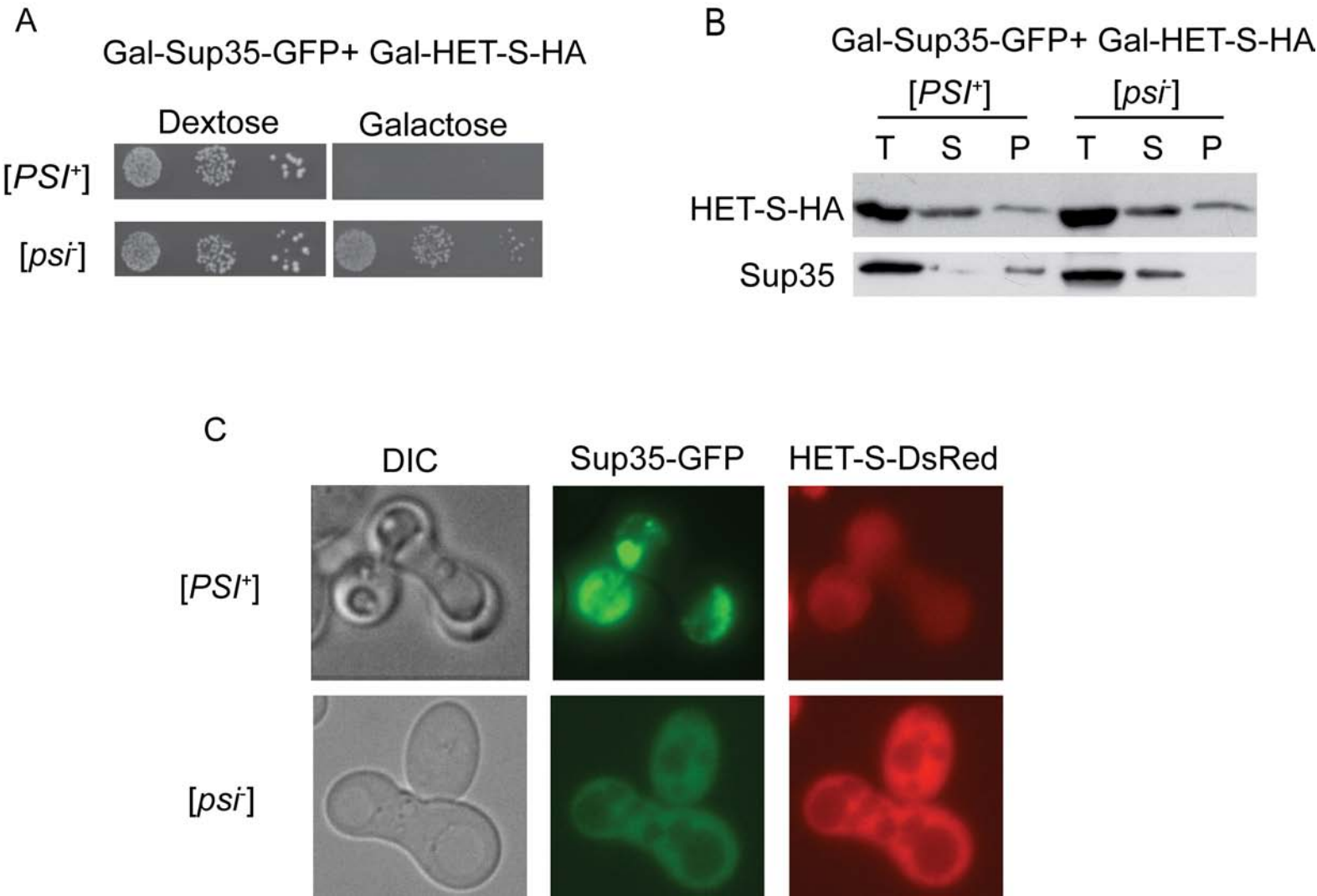
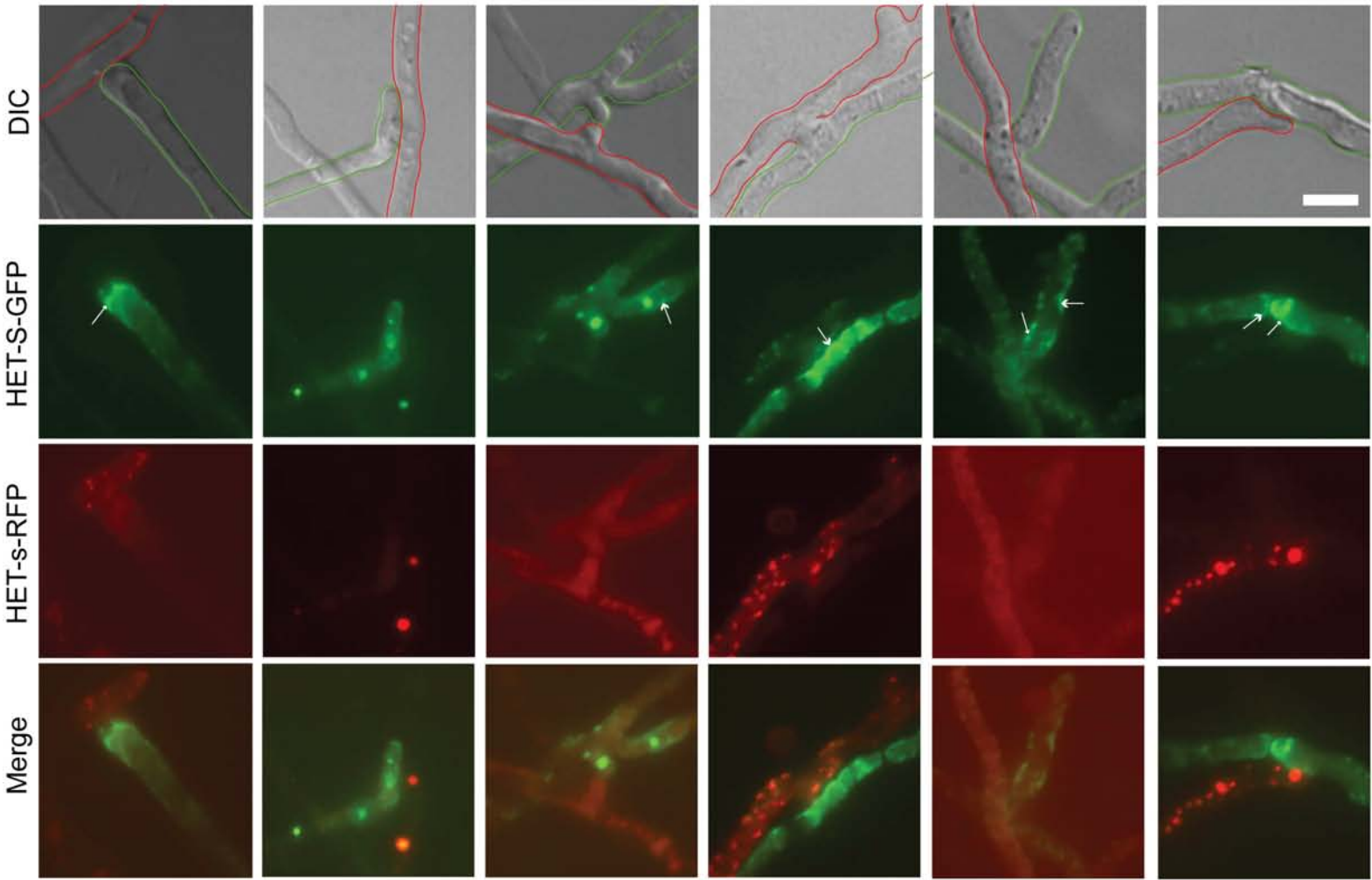


Figure 7

A



B

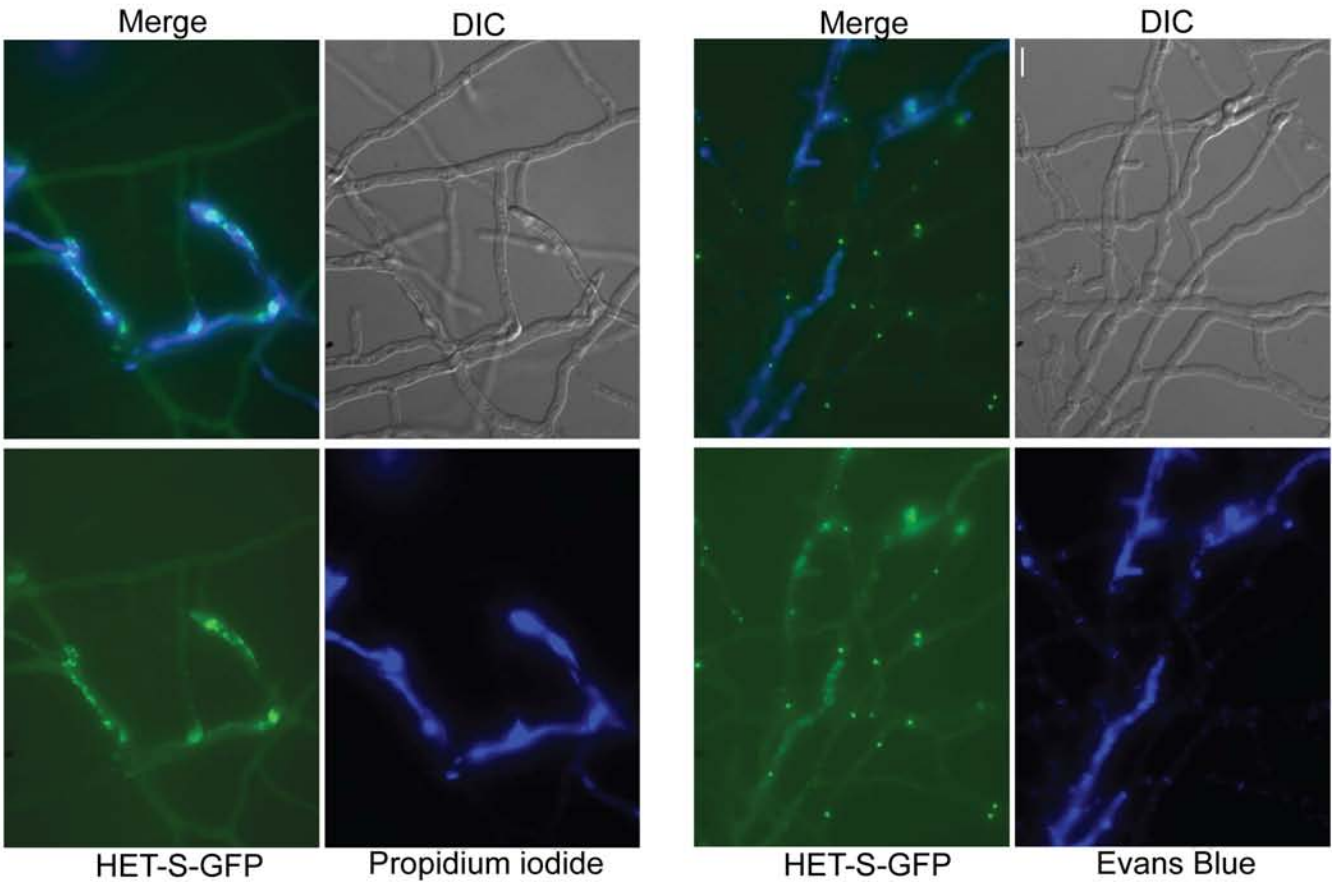


Figure 8

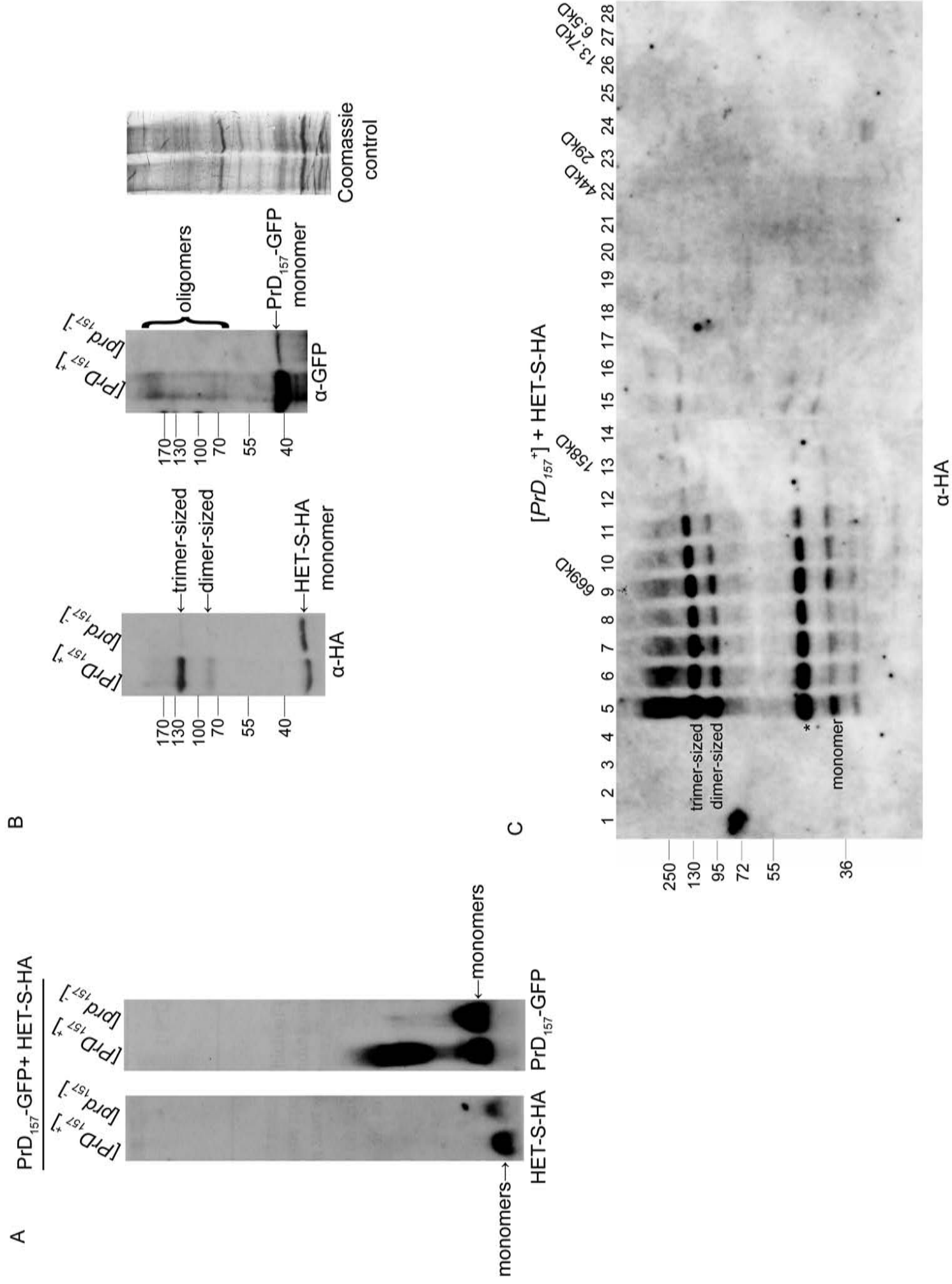
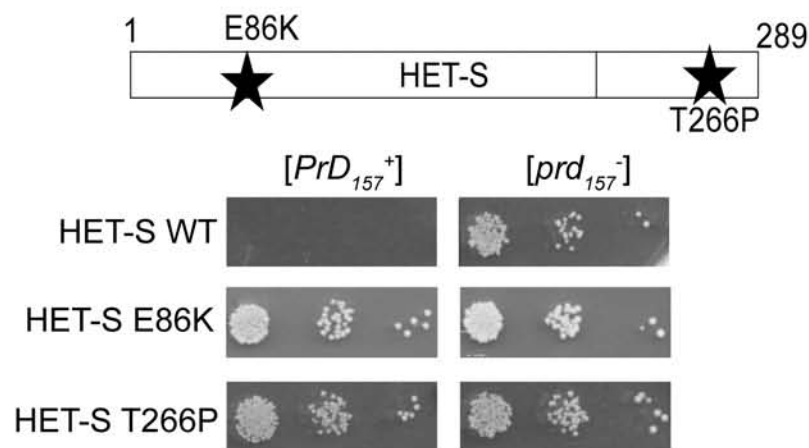
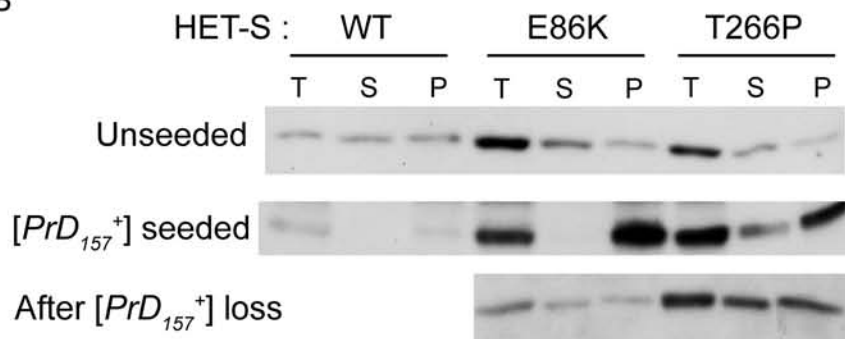


Figure 9

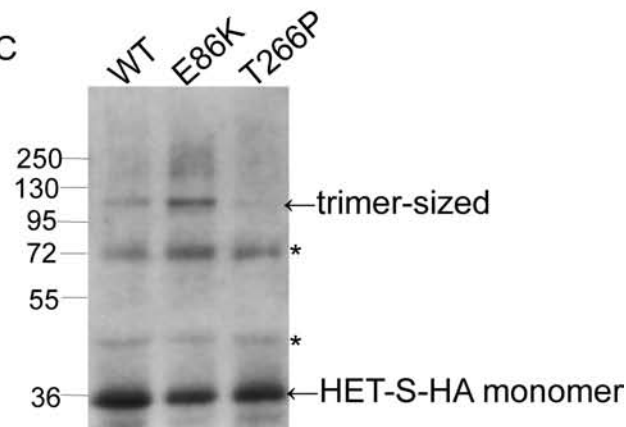
A



B



C



D

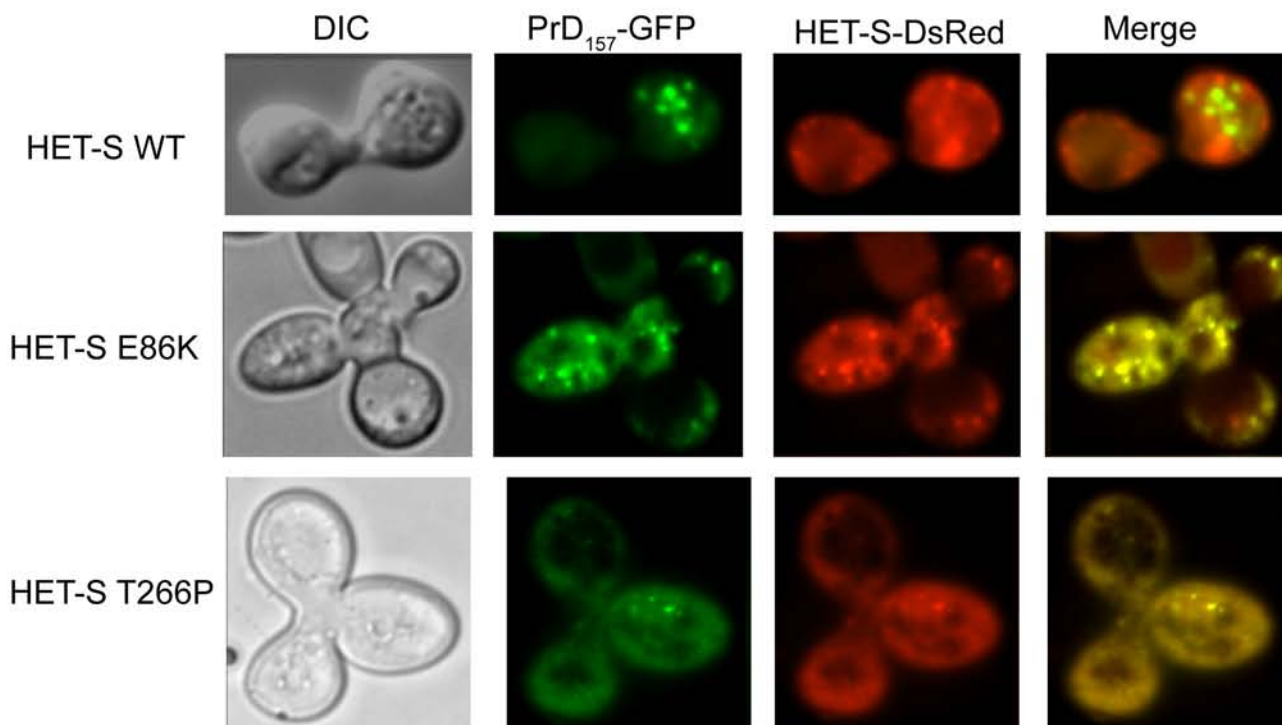
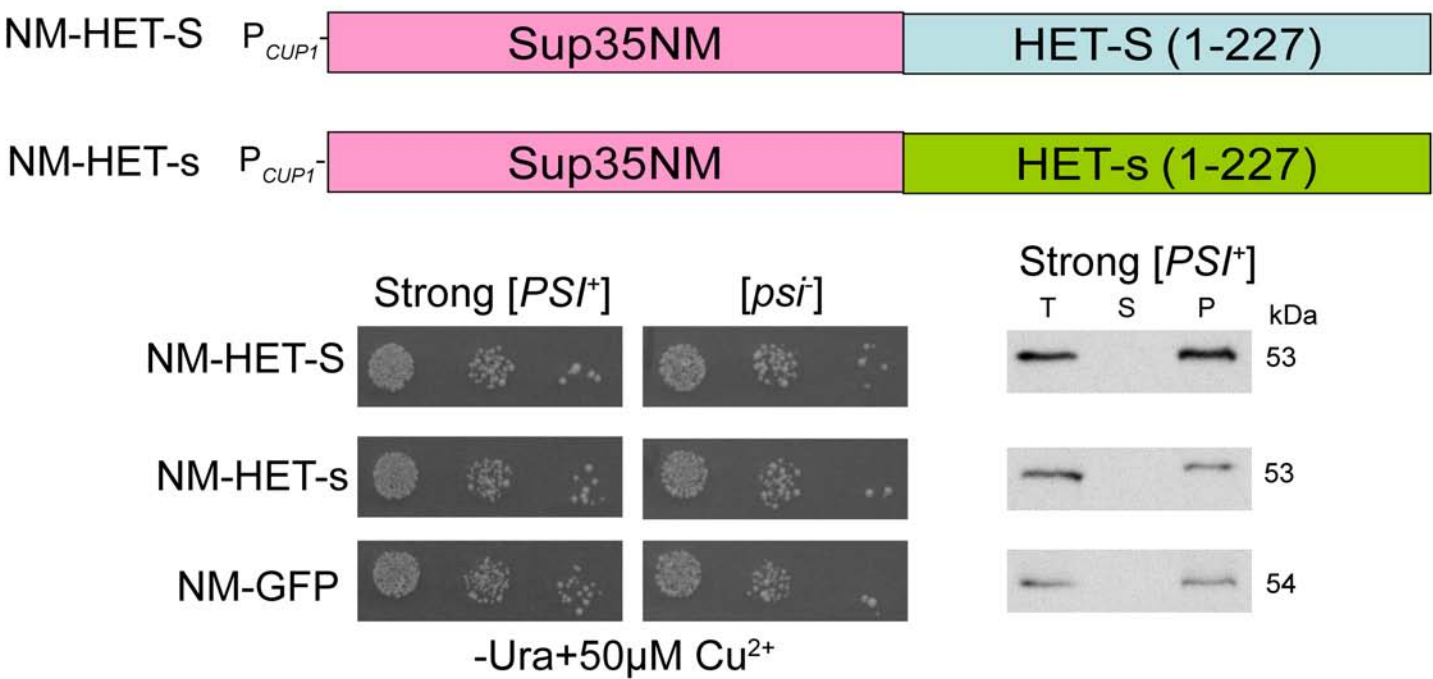


Figure 10

A



B

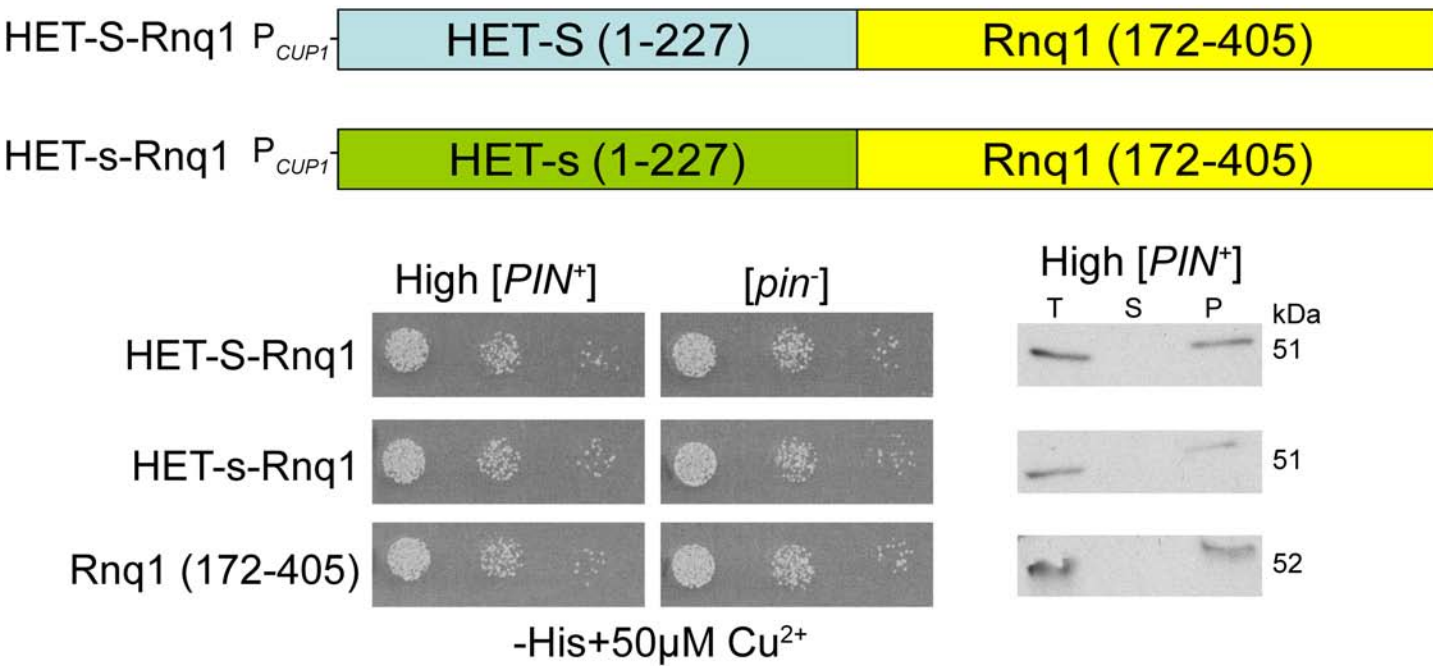
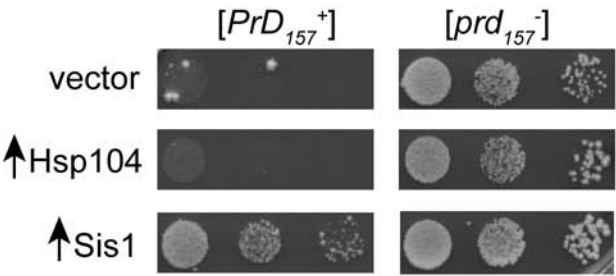
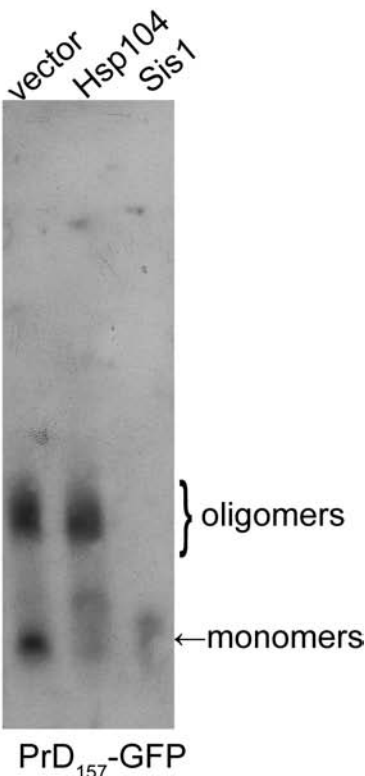


Figure 11

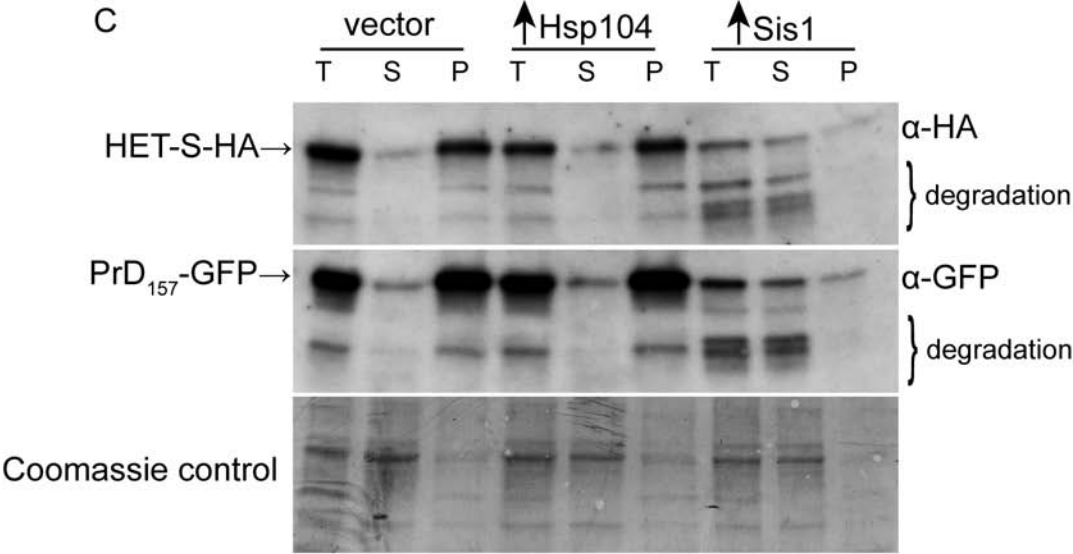
A



B



C



D

